Volume 37, Issue 01, 2024 ISSN 1096-9411 (print) / 2769-822X (online)

Dental Anthropology

A Publication of the Dental Anthropology Association

Dental Anthropology

Volume 37, Issue 01, 2024

Dental Anthropology is the Official Publication of the Dental Anthropology Association.

Contact for Manuscripts

Rebecca L. George

Western Carolina University

E-mail address: rgeorge@wcu.edu

Website: journal.dentalanthropology.org

Published at

University of Nevada, Reno

&

Western Carolina University

Variation in Regional Enamel Growth Rates in Modern Humans Presenting Dental Evidence of Vitamin D Deficiency

Christopher Aris, [1,2*+] Katie A. Hemer, [1,3+] and Emma Street [4]

[1] Department of Archaeology, University of Sheffield, UK
[2] School of Chemical and Physical Sciences, Keele University, UK
[3] Institute of Archaeology, University College London, UK
[4] No affiliation

Keywords: Vitamin D, dentine, enamel, daily secretion rates

ABSTRACT
Introduction: Enamel development (amelogenesis) research has been fundamental to our understanding of variation in human enamel physiology. However, research into internal enamel structures is often limited to exploring rates of enamel formation. This study addresses this gap by analysing enamel growth and the impact metabolic disease can have on that growth.
Materials and methods: Thin sections were produced for nine permanent teeth, five presenting zero or minimal evidence of vitamin D deficiency, and four presenting moderate-severe deficiency. Vitamin D deficiency was identified via interglobular dentine (IGD). Enamel development was analysed through daily secretion rates (DSRs). Statistical analysis investigated for variation in mean DSRs, and overall DSR distribution variance, across mid, inner, and outer lateral enamel regions between IGD-absent and IGD-present groups.
Results: Mean DSRs were significantly faster in the inner and mid regions in the IGD-present group. Distribution variance was significantly larger in all regions in the IGD-present groups.
Conclusions: These findings suggest that vitamin D deficiency impacts the formation of enamel concurrently with dentine. While more research into the correlation between IGD formation and changes in DSRs is needed, these findings allude to vitamin D deficiency regulating human enamel secretion and/or enamel undergoing catchup growth after vitamin D deficiency recovery comparable to bone.

Human enamel growth rates are frequently analysed through histological analysis within the fields of biological anthropology and bioarchaeology. Such analyses have primarily focused on the variation between cusps of the same tooth (e.g., Mahoney, 2008), within individual populations (e.g., Schwartz, Reid, and Dean, 2001), as well as comparison between different populations (e.g., Smith et al., 2007**;** Aris et al., 2020a, 2020b). Whilst the scope of research into enamel growth variation between groups has been wide, these projects have almost exclusively researched dental samples presenting no evidence of pathology or stress markers such as linear enamel hypoplasia. Select research has commented on how other human enamel growth features have varied between groups of individuals not suffering from physiological stress compared to those that were under stress, as identified from dental evidence; these studies have, however, typically focused on the influence of the methodologies used to calculate enamel growth across different tooth types (e.g., Lukacs and Guatelli-Steinberg, 1994; Guatelli-Steinberg and Lukacs, 1999; FitzGerald and Saunders, 2005). Indeed, relatively limited research has been published which directly considers the relationship between permanent enamel growth and stress. This includes studies such as those identifying slowing enamel formation rates after birth in deciduous teeth (Birch and Dean, 2009), and those whose data could be interpreted as showing drops in enamel formation rates potentially related to seasonal stressors (Macchiarelli et al., 2006). More recently, Aris and Street (2021) analysed growth rates of accessory enamel (defined by them as "growth of enamel outside of the features typically used to define and identify human tooth types"),

+ These authors contributed equally
*Correspondence to:
Christopher Aris
Keele University
Email: c.aris@keele.ac.uk

and found that the presence of accessory enamel growth correlated with a significant slowing of enamel growth within the normal enamel areas of the same tooth, and compared to 'normal' teeth from the same population. This evidence suggests that not only is there scope to further investigate the correlation between normal and accessory enamel growth in other populations, but there is also a need to consider the relationship between other dental defects and pathologies which could significantly influence the growth rates of human enamel. Interglobular dentine (IGD), often appearing as zones of black globular patches within the dentine, is an example of a defect observable in the same tooth cross sections used for collecting enamel growth data (e.g., Nanci and Smith, 2020; Snoddy et al., 2020). The presence of IGD has been linked to vitamin D deficiency at the time of dentinogenesis (e.g., Kagayama et al., 1997; Tsuchiya et al., 2002). By analysing teeth presenting IGD and those that do not from the same population, we can begin to examine whether dental enamel growth rates are influenced by vitamin D deficiency. It is further possible to use the specific location of IGD to identify whether any variation in tooth enamel growth between deficient and non-deficient individuals is regional within the tooth, since IGD has been shown to appear at different foci within the tooth crown and root (Jayawardena et al., 2009). This analysis will help inform our understanding of how tooth enamel growth rates vary in individuals presenting dental manifestations of pathology, and specifically the potential disruption to enamel growth caused by a metabolic condition, such as vitamin D deficiency.

Background

Amelogenesis and Daily Enamel Growth

Ameloblast cells secrete and mineralize protein matrix in a process known as amelogenesis (Boyde, 1989; Nanci and Smith, 1992; Smith and Nanci, 2003). During the amelogenesis stage in which the matrix is secreted, the behaviour of ameloblasts is altered according to a circadian rhythm, which produces short-period markers along the length of enamel prisms; these line markers are referred to as cross-striations (e.g., Boyde, 1963; 1990; Massler and Schour, 1946; Okada, 1943; Kajiyama, 1965; Dean et al., 1993; Dean, 1995; Antoine, 2001; Smith and Nanci, 2003; Antoine et al., 2009). Cross-striations possess a different refractive index to that of the rest of the volume of enamel prisms thus making them visible in dental thin sections using transmitted light microscopy (e.g., Berkovitz et al., 2002; Zheng et al., 2013).

By counting cross-striations, daily enamel secretion rates of enamel matrix (DSRs) can be calculated (Aris, 2022). Research on teeth without pathology or abnormal growth variations show DSRs to accelerate from inner to outer enamel regions, along the pathway of enamel prisms, from the enamel dentine junction (EDJ) towards the outer enamel surface (e.g., Beynon, Dean, and Reid, 1991; Beynon et al., 1998; Reid, Beynon and Ramirez Rozzi, 1998; Lacruz and Bromage, 2006; Mahoney, 2008; Aris et al., 2020a, 2020b; Aris and Street, 2021). Further variation in DSRs has been observed along the EDJ, with faster rates recorded with increased proximity to the dentine horn (Beynon, Dean, and Reid, 1991). As a result of DSRs varying within a tooth, both along and away from the EDJ, their analysis often involves calculating them for defined areas of the tooth crown: cuspal, lateral, and cervical enamel, which are then subdivided into inner, mid, and outer regions (e.g., Aris et al., 2020a, 2020b).

The relationship between enamel growth patterns, stress and pathology

While teeth presenting evidence of pathology or stress have been relatively absent from studies of enamel DSRs, different features of enamel growth have been investigated in dentition, especially in teeth showing physiological signs of stress (e.g., Lukacs et al., 1989; Lukacs, 1991, 1992, 1999; Lukacs and Joshi, 1992; Lukacs and Pal, 1993; Lukacs and Guatelli-Steinberg, 1994; Goodman and Song, 1999; Lukacs and Walimbe, 1998; Guatelli-Steinberg and Lukacs, 1999; Holt, Reid, and Guatelli-Steinberg, 2012; Birch and Dean, 2014). Much of this research has focused on the aetiology of external enamel growth defects via the impact of physiological stress on amelogenesis. For example, a series of papers have been published by Lukacs and colleagues on the pattern and expression of enamel defects in modern human populations (Lukacs et al., 1989; Lukacs, 1991, 1992, 1999; Lukacs and Joshi, 1992; Lukacs and Pal, 1993; Lukacs and Guatelli-Steinberg, 1994; Lukacs and Walimbe, 1998; Guatelli-Steinberg and Lukacs, 1999). Their results show that the expression of such defects, such as enamel hypoplasia, can vary between groups as a result of differing geographic location, climate, and diet. Of greatest significance to this study is that these articles also found evidence of increased crown formation times (CFTs) in individuals presenting stress-induced enamel defects. Further studies have subsequently been published, and have all further stated that when physiological stress impacts enamel structures it significantly increases CFTs (e.g., Holt, Reid, and Guatelli-Steinberg, 2012; Birch and Dean, 2014; Primeau et al., 2015). Crown formation times, as a measure of enamel growth utilising cross striations, are directly related to other measures of enamel growth including DSRs (e.g., Massler and Schour, 1946). Therefore, if physiological stress can influence CFTs, it is reasonable to assume that physiological stress caused by nutritional deficiencies may also impact enamel matrix DSRs.

The potential to use enamel defects to predict the precise age at which a stressful event occurred has improved the way that we can investigate the impact of stress on enamel growth; this is possible due the regular, daily process by which cross-striations are formed (e.g., Antoine, 2001; FitzGerald and Saunders, 2005; Antoine et al., 2009). When cross-striations are altered, the ability to calculate the timing of these alterations can be correlated with when the individual is likely to have experienced the stressful event. Using a large sample of 274 teeth from 127 Roman subadults, FitzGerald and Saunders (2005) postulated that enamel formation is proportionally impacted in relation to the severity of the stressful event. They further concluded that there is no minimum level of stress required for enamel growth to be affected (FitzGerald and Saunders, 2005). It is therefore plausible that nutritional stress, such as that impacting on dentine formation, could equally impact on enamel growth.

Aris and Street (2021) expanded the research into DSRs by investigating the growth of accessory and non-accessory enamel presented in a modern-day incisor with a talon cusp. Their findings suggested that the presence of accessory enamel resulted in an overall slowing of enamel growth across the enamel cap. The exact aetiology of talon cusps is thought to be genetic, with predisposition to accessory cusp development further increased through stress and/or trauma during the development of the dental papilla (e.g., Mohan et al., 2013; Kalpana and Thubashini, 2015). This finding further shows how stress and/or genetically-determined pathological cases of dental manifestations have the potential to influence enamel growth. Furthermore, Aris and Street (2021) conclude that the lack of research on DSRs in association with different dental defects limits the overall understanding of how stress and pathology affects enamel growth, and whether that is always the case. Analysis of regional DSRs alongside the presence of IGD, as a marker of vitamin D deficiency, will work to address this.

Vitamin D

Vitamin D is essential for regulating calcium homeostasis within the human body; without the hormone, the body is unable to effectively absorb calcium and phosphate from the intestines and this results in the skeleton's inability to mineralize osteoid, that is, the precursor to bone (Holick, 2007; Brickley and Ives, 2008). Whilst dietary sources of vitamin D are available (e.g., oily fish, eggs), for most individuals, cutaneous synthesis is the main source of vitamin D. Vitamin D is synthesised following the exposure of the skin to ultraviolet B (UVB) radiation which creates the pre-hormone vitamin D3 (cholecalciferol). Vitamin D3 is inert, and therefore goes through a two-stage process to convert it into its biologically active form; this first step occurs in the kidneys, and then subsequently in the liver. It is the active form of vitamin D (1,25 (OH)2D) that is responsible for the absorption of calcium and phosphate from the blood (Nair and Maseeh, 2012).

The active form of vitamin D plays a significant role in most tissues within the body by binding to vitamin D receptors (VDR) in target cells (Holick, 2007). These vitamin D receptors (VDR) bind to specific regions of nuclear DNA known as vitamin D response elements (VDRE), and in doing so regulate the expression of more than 900 genes responsible for a variety of different physiological functions (Berdal et al., 1995; Bailleul-Forestier et al., 1996; Kongsback et al., 2013; Botelho et al., 2020). The VDR are therefore essential for regulating homeostatic processes, in particular by increasing the efficiency of calcium and phosphate absorption (Holick, 2007). This is especially true in the mineral-regulating organs such as the kidneys and intestines, as well as in bones and teeth where VDR are found in the bone-forming osteoblast cells (Dowd and MacDonald, 2013: 540; Keller & Wahli, 1997: 283).

A disruption to the synthesis of Vitamin D and inadequate calcium absorption can result in metabolic bone diseases due to its impact on bone osteoid. Osteoid is the precursor to bone formed by osteoblasts during growth and bone remodelling; during bone mineralisation, calcium phosphate nanocrystals populate a collagen-based organic matrix in order to create bone's dense structure (Brickley, Moffat, and Watamaniuk, 2014; Kuhn, 2001). Without adequate calcium phosphate, the osteoid remains unmineralized. As a consequence, in the growing skeleton, defects in the bone at the sites of endochondral growth occur, including porosis, disorganised bone, and the splaying of the bone under mechanical force. The outcome includes the formation of bending deformities such as bowed limbs, deformation, and pseudofractures (Brickley and Mays, 2019).

Vitamin D deficiency and Interglobular dentine (IGD)

Whilst changes to the skeleton may be observed macroscopically, vitamin D deficiency also has an impact on the formation of dentine during tooth development. During the early stages of dentinogenesis, dentine - a proteinaceous calcified tissue - is formed by the action of odontoblast cells. It commences at the point where the tooth germ reaches the late bell stage; in first permanent molars, the formation of the cuspal dentine, the horns, begins in-utero at around 30 weeks gestation (Hillson, 1996: 122). Mantle dentine is formed first near the dentino-enamel junction, whilst circumpulpal dentine subsequently forms beneath the mantle (Kagaymama et al., 1997: 477-78). Dentine is laid down in an incremental fashion through the activity of the odontoblast cells which go through a process of cell differentiation, as well as the secretion of a collagen matrix, and the mineralisation of the matrix through the coalescence of spherical hydroxyapatite crystals (calcospherites) (Jayawardena et al., 2009; Opsahl Vital et al., 2012). In a vitamin D sufficient individual, who has adequate calcium and phosphate blood serum levels, the calcospherites fuse to form a homogenous mineralised dentinal matrix (Jayawardena et al., 2009; Opsahl Vital et al., 2012). If an individual is vitamin D deficient, however, the mineralisation of the dentine is disrupted and the calcospherites fail to grow and coalesce leaving behind bands of dark voids; these are areas of unmineralised dentine known as interglobular dentine (IGD) (Jayawardena et al., 2009; Opsahl Vital et al., 2012; D'Ortenzio et al., 2016: 152-153) (Figure 1). Through the histological analysis of teeth, it is possible to identify those individuals who experienced a single episode of vitamin D deficiency (represented by a single band of IGD), or multiple episodes of vitamin D deficiency (represented by more than one band of IGD), during tooth dentine formation. Bioarchaeological studies have linked the presence of IGD to skeletal changes indicative of vitamin D deficiency rickets in archaeological populations (e.g., D'Ortenzio et al., 2016; Veselka et al., 2019; Hemer and Verlinden, 2020), yet no studies have sought to identify a link between vitamin D deficiency and enamel growth rates, as proposed here.

Figure 1. Thin section of the first permanent molar from Skeleton 278. Two bands of IGD are indicated by the white, star-shaped markers; these suggest this individual experienced two separate episodes of vitamin D deficiency within the first three years of life.

Materials and Methods

Dental sample

Teeth were sampled from an archaeological population from southwest Wales dating from the 8th-11th century AD. The sampled individuals form part of a wider bioarchaeological research project into the population led by KH. Preliminary analysis of a single juvenile skeleton from the site revealed skeletal and histological evidence for vitamin D deficiency rickets (Hemer and Verlinden, 2020); further investigation is ongoing to explore the impact of this metabolic condition on the wider population. Before destructive sampling of the teeth was undertaken, all individuals were subjected to a rigorous, macroscopic osteological assessment following the recommended guidelines of the British Association for Biological Anthropology and Osteology (Brickley and Mckinley, 2004) and the Chartered Institute for Archaeology (Mitchell and Brickley, 2017). Each skeleton was recorded including their degree of preservation, an estimation of age, sex, and stature (where possible), and any skeletal markers of physiological stress, disease, and trauma were also recorded.

Sample preparation

Histological thin sections were produced using standard procedures for dental sampling (e.g., Schwartz et al., 2005; Mahoney, 2008; Aris, 2020). Each tooth was embedded before cutting in a resin-hardener mixture (Buehler®) in order to reduce the chance of any enamel fracturing during the sectioning process. Embedded samples were then cut at a low speed using a diamond-edged wafering blade (Buehler® IsoMet 1000 Precision Cutter) at a longitudinal angle through the apex of the selected cusp (see below). The samples were then mounted on glass microscope slides and lapped using progressively finer grinding pads (Buehler®) until the dental material was around 100-120μm thick. Ground samples were polished using 0.3μm aluminium oxide powder to improve the clarity of the slides during microscopy. Polished samples were then placed within an ultrasonic bath for two minutes in order to remove any remaining debris before being dehydrated using 90% and 100% ethanol-based solutions (Fisher scientific®). All sections were examined using polarised light microscopy (Lecia DM2700 P system microscope). Analysis and image capture was conducted using micro imaging software (Leica microsystems LAS v4) (see below for detail).

Daily secretion rates

Daily secretion rates (DSRs) were calculated for the inner, mid, and outer areas of the lateral enamel region of each tooth using standard methods (e.g., Beynon, Dean, and Reid, 1991; Schwartz et al., 2001; Mahoney, 2008; Aris et al., 2020a, 2020b). Each section of the three areas was determined by dividing the length of the lateral enamel region into three equidistant portions, following the longitudinal axis of local enamel prisms (Figure 2). The lateral enamel region itself was determined within the section of imbricational enamel equidistant between the dental cervix and dentine horn. For molars, DSRs were collected from the lateral regions of buccal cusps, and for canines from the labial enamel. This approach was selected due to its prevalence in human enamel DSR studies, and for the fact that it accounts for any inter-prism pathway variation occurring within regional areas of the enamel cap.

In order to fully appreciate any difference in enamel formation rates across the enamel cap, and for each tooth type, the time periods between each isolated region were calculated. This was done using measured lateral enamel thickness (as per Aris, 2022) and the proportion of this separating each region (as above) and dividing them by regional DSRs (see below; e.g., Smith et al., 2003; Mahoney, 2008). This can be done with more precision by following single enamel prisms and counting the cross striations along the length of the space separating each region (e.g., Mahoney, 2011). Unfortunately, this approach was not possible for this study due to the level of diagenesis making counting cross striations over relatively long internal enamel cap distances impossible.

Within each enamel region a measurement was made of five consecutive cross striations along the length of an enamel prism. This measurement was subsequently divided by five, giving a mean daily rate of matrix secretion (μm/day). This process was repeated to produce six mean DSRs for each region. In previous studies, these six regional means have been averaged again to give a 'grand mean' (e.g., Beynon, Dean, and Reid, 1991; Beynon, Clayton, and Ramirez Rozzi, 1998; Reid, Beynon and Ramirez Rozzi, 1998; Lacruz and Bromage, 2006; Mahoney, 2008; Aris et al., 2020a, 2020b). This approach was, similarly to regional separation, due to its prevalence in human enamel DSR studies (e.g., Mahoney, 2008; Aris et al., 2020a, 2020b; Aris, 2022) and to help account for any local variation between different enamel prism pathways. In preliminary studies using smaller sample sizes, the six

Figure 2. Digital images of a first molar and canine cross section displaying the locations from which lateral enamel regions were defined. The smaller green rectangles highlight the lateral areas from which DSRs were collected, and the larger green rectangle a representation of how inner, mid, and outer regions (moving left to right) were isolated.

mean DSRs for each region are, instead, used individually in analyses to better represent the variability of DSRs within enamel cap regions (Aris and Street, 2021). As a result, the six mean DSRs for each region of each tooth analysed here were kept separate and not used to form a 'grand mean'. All cross striation measurements were taken at 20x magnification (Figure 3).

Interglobular dentine

The ten histological thin sections were observed microscopically, and IGD was recorded as present or absent. In those cases where IGD was present, the scoring system of D'Ortenzio et al. (2016: 157) was employed in order to score the degree of severity according to their classification system of Grades 0 – 3, with Grade 0 representing normal dentine without IGD present, and Grade 3 representing the most severe manifestation of IGD including many large, interglobular spaces with a distinctive scalloped appearance covering >75% of the area of interest. Consideration was also given to the location of the IGD and the method of D'Ortenzio et al. (2016) was used to estimate the age/ages – represented by multiple bands of IGD – at which the individual experienced a deficiency in vitamin D and disruption of calcospherite growth occurred.

Statistical analysis

Mann-Whitney tests were run in order to identify any differences between the DSRs of equivalent regions from the IGD-present and IGD-absent groups. Subsequent F-tests were also conducted for each equivalent region in order to identify whether there was any significant difference between the variance in the distribution of DSRs between the two groups. Boxplots and descriptives were also produced to investigate any variation occurring between the tooth types analysed, in case this may have influenced the identification of any differences between the pooled IGD-present and IGD-absent groups. All statistical analyses were performed using SPSS 26.0.

Figure 3. Digital image of an isolated enamel region displaying cross striations, captured at 40x magnification. Clusters of white arrows display how groups of adjacent cross striations were used for DSR calculations.

Results

Interglobular dentine

Of the ten teeth subjected to a microscopic assessment, six presented evidence of IGD (Table 1). There was variability in the severity of the IGD present, with most teeth exhibiting Grade 1 or Grade 2 severity, whilst only one case exhibited severe IGD which impacted >75% of the area relative to the amount of normal dentine. Whilst most teeth have a single band of IGD, representing a single influential episode of vitamin D deficiency, two teeth (belonging to STP 278 and STP 245) both exhibited two distinct bands of IGD occurring on two separate occasions during dentine formation. In skeleton STP 278, the first episode of disruption to the dentine formation occurred between 6 and 18 months of age, whilst the second band of IGD suggests another episode of disruption to dentine formation between 2 and 2.5 years of age (Hemer and Verlinden, 2020: 10). In skeleton STP 245, two bands of IGD were present; the first band / episode occurred within the first 6 months of life, whilst the second band / episode occurred between 6 and 18 months of age. Overall, the sample represents a high proportion of individuals whose dentinogenesis was disrupted by inadequate vitamin D synthesis.

Daily secretion rates

Table 2 shows the results of the Mann-Whitney U and F-tests for differences between group mean regional DSRs and group DSR distribution respectively. The Mann-Whitney U tests identified significantly faster DSRs in the IGD-present group for the inner (p=0.03) and mid (p=0.05) enamel region. While the difference was not significant between the group outer regions, mean DSRs were still faster in the IGD-present group by 0.17μm compared to the IGD-absent group - a mean difference equal to that observed in the inner and mid enamel region data (Figure 4). In contrast the F-tests identified significant differences for all enamel regions, with significantly larger variance in DSRs observed across the whole enamel cap in the IGD-present group compared to the IGD-absent group (inner: p<0.01; mid: p=0.05; outer: p<0.01).

Table 3 shows (with Figures 5 and 6 visualising) the DSR distribution for un-pooled tooth type samples for both the IGD-present and IGD-absent groups (respectively). While the deviation between the canines and molars in the IGD-present group appears notable, this is likely due to the disproportionate sample sizes (see Table 3), and in fact the mean values are relatively consistent - varying consistently by <0.5μm in all enamel regions. Even less

Table 1. Samples analysed including the presence/absence and severity of IGD recorded for each tooth.

Sampled Skeleton	Tooth analysed	IGD Present / Absent	# IGD episodes	Severity of IGD
STP 262	L. Max. Canine	Absent	0	N/A
STP 240	L. Max. Canine	Absent	0	N/A
STP 206	R. Max Canine	Absent	0	N/A
STP 242	L. Max M1	Absent	0	N/A
STP 216	L. Max M1	Present	1	Grade 1
STP 261	R. Man. Canine	Present	1	Grade 1
STP 245	L. Max M1	Present	2	First IGD band - Grade 2 Second IGD band - Grade 1
STP 278	L. Man M1	Present	2	Both IGD bands - Grade 2
STP 218	R. Max M1	Present	1	Grade 2
STP 257	L. Max M1	Present	1	Grade 3

Table 2. *Results of the Mann-Whitney and F-tests for variations in regional mean DSRs (µm/day) between the IGD-present and IGD-absent groups. Significant results are marked in bold, p < 0.01.*

Region	IGD group	N	Mean	SD	Min	Max	F	Mann-Whitney U test Sig.	F-test Sig.
Inner	Present	24	1.9	0.34	1.38	2.6	4.63	**0.03**	**0.00***
	Absent	30	1.73	0.2	1.39	2.23			
Mid	Present	24	2.13	0.28	2.13	2.64	3.93	**0.05**	**0.05**
	Absent	30	1.96	0.33	1.57	2.82			
Outer	Present	24	2.32	0.55	1.53	3.7	1.84	0.18	**0.00***
	Absent	30	2.15	0.31	1.6	2.79			

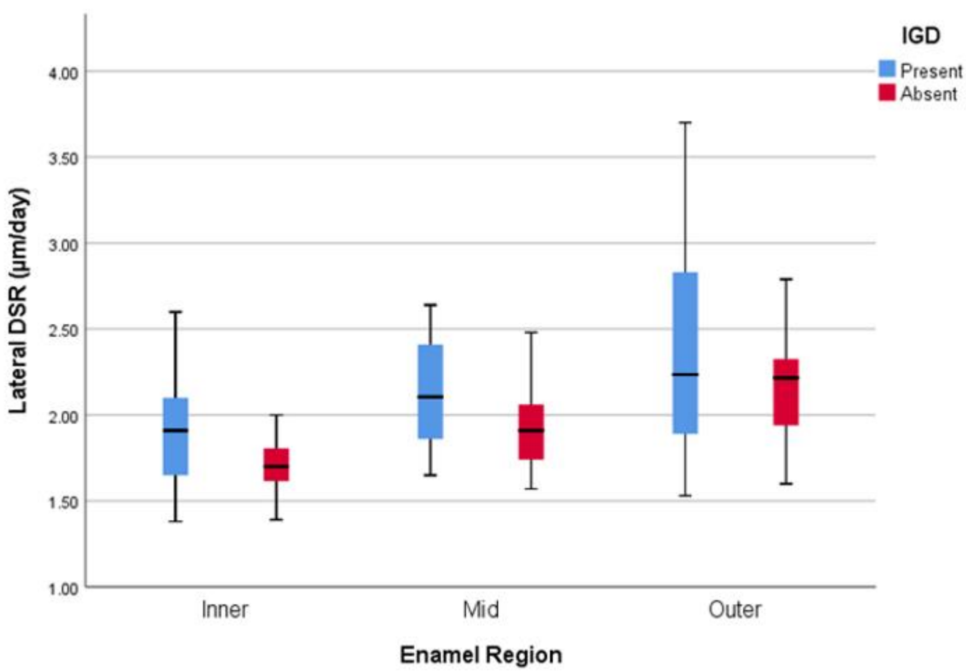

Figure 4. Plot of DSR data distribution of each sample group and enamel region. The central line displays the mean DSR value for the associated group and region.

Table 3. Descriptive statistics for regional mean DSRs (µm/day) for canine and molar split for the IGD-present and IGD-absent groups.

Region	IGD group	N	Mean	SD	Min	Max
			Molars			
Inner	Present	24	2.07	0.29	1.56	2.60
Mid	Present	24	2.20	0.27	1.65	2.64
Outer	Present	24	2.43	0.57	1.53	3.70
			Canines			
Inner	Present	6	1.49	0.10	1.38	1.66
Mid	Present	6	1.83	0.01	1.81	1.86
Outer	Present	6	1.91	0.04	1.86	1.97
			Molars			
Inner	Absent	12	1.83	0.23	1.39	2.23
Mid	Absent	12	2.07	0.40	1.60	2.82
Outer	Absent	12	2.19	0.41	1.60	2.79
			Canines			
Inner	Absent	12	1.63	0.10	1.41	1.79
Mid	Absent	12	1.85	0.20	1.57	2.26
Outer	Absent	12	2.11	0.14	1.84	2.29

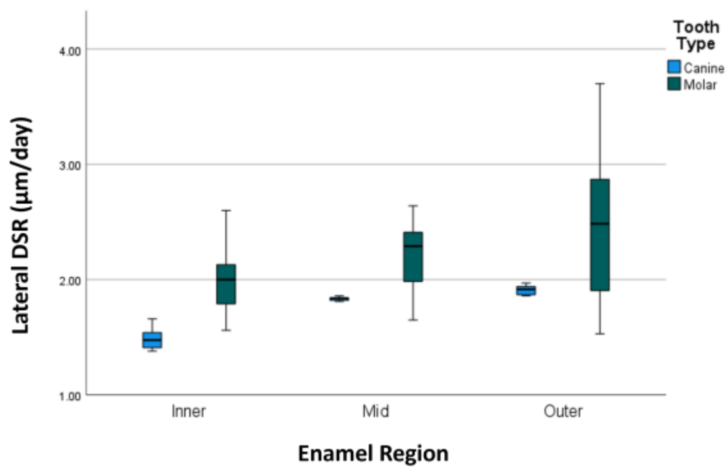

Figure 5. Plot of DSR data distribution for the IGD-present groups of the canines and molars. The central line displays the mean DSR value for the associated group and region.

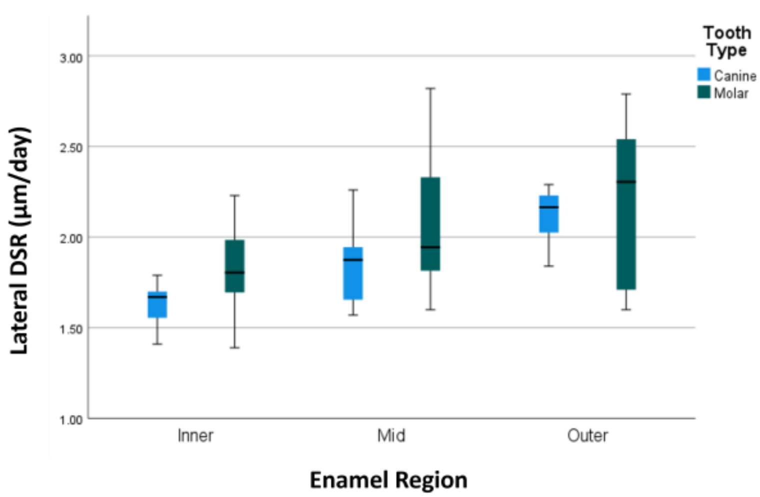

Figure 6. Plot of DSR data distribution for the IGD-absent groups of the canines and molars. The central line displays the mean DSR value for the associated group and region.

variation can be observed between the IGD-absent canine and molar groups, with consistently ≤0.3μm difference between regional mean DSRs. Even less variation was observed in the deviation in this group also, however this was likely due to the sample sizes being equal between tooth types when split in this way.

Inter-enamel region formation time
Inter-enamel region formation times were calculated by dividing proportional quantities (see Figure 2) of the total lateral thickness (LT) of the corresponding enamel region by the mean regional growth rates. The mean LT of the canines was 1.12mm, and the mean LT of the molars was 1.48mm - both comparable to LT values of multiple analysed human populations (Aris, 2022). Moreover, LT values did not vary by any notable measure between the IGD-present and IGD-absent groups, suggesting no impact of total enamel thickness as a result of vitamin D deficiency. Lateral enamel formation periods all overlapped with IGD formation periods (6-18 months; see Section 3.1) although some variation between sample groups was noted (see below).

For IGD-present molars inner, mid, and outer regions represented 236, 222, and 201 days of growth respectively - suggesting just under two years total lateral enamel formation time. For IGD-present canines inner, mid, and outer represented 248, 202, and 193 days respectively - suggesting again a formation time of just under two years.

For IGD-absent molars inner, mid, and outer regions represented 267, 236, and 223 days of enamel secretion respectively - suggesting roughly two years of total lateral enamel formation time. For IGD-absent canines the inner, mid, and outer regions represented 226, 200, 175 - suggesting around 18 months of total lateral enamel formation.

Discussion
With the exception of outer lateral enamel matrix DSRs, enamel growth measures were found to vary significantly across multiple factors between the IGD-present and IGD-absent samples. While the initial analysis indicates that the presence of IGD correlates with faster enamel growth and potential 'catch-up growth' in teeth similar to bone (e.g., Mays et al., 2009; Rajah et al., 2008), additional analysis instead suggests that the significant variations are a result of a drastically larger distribution of growth rates across the lateral enamel of IGD-present teeth. While it is plausible that some variation may be the result of multiple tooth types being analysed, the comparative analysis here suggests this is minimal (although future research should consider analysing this with larger sample sizes). Moreover, lateral enamel formation times for the IGD-present samples was near-identical between the tooth types, suggesting reliable combination of DSRs for these groups - although there was more notable difference in formation times between IGD-absent groups (discussed more below). Overall, this all alludes to a potential interruption of standard enamel growth patterns which is likely caused by the same interference arising from vitamin D deficiency and the incomplete formation of dentine.

Inter-group equivalent region analysis
The mean lateral DSRs were significantly faster in the IGD-present teeth for the inner and mid regions alluding to potential catch-up growth later in the development of the dentition. Such variations between the growth of equivalent enamel regions are not uncommon, and those seen here are comparable to similar differences which have been observed both within and between groups from British populations (Aris et al., 2020a, 2020b). However, within the context of analysing dentition showing evidence of pathology/nutritional deficit, this finding is unexpected yet is supported by the lateral enamel formation time analysis, which found notably shorter formation times in the IGD-present molar group compared to the IGD-absent molar groups - again indicating faster enamel growth in a number of the IGD-present samples. The research which has been conducted in the past has found links between physiological stress and the slowing trajectory of enamel cap formation (e.g., Reid and Dean, 2006; Holt, Reid, and Guatelli-Steinberg, 2012; Birch and Dean, 2014; Primeau et al., 2015), and thus it would be reasonable to expect to see slower DSRs in IGD-present groups.

Moreover, recent research on accessory enamel growth has found evidence of enamel defects being more influential on the trajectory and pattern of enamel DSRs, rather than simply reducing the speed of enamel development (Aris and Street, 2021). It is therefore possible that the variations observed here could suggest that DSRs and CFTs can vary independently according to different external factors. Similar suggestions have been made to this effect in the past, with the additional discussion of enamel thickness (Aris et al., 2020b). What remains potentially unexplained by the analysis of mean DSRs however, is why the outer region displayed no significant difference between the IGD-present and IGD-absent groups, while the difference in mean was the same for all three equivalent region comparisons (0.17µm/day), and graphically appearing as the most variable region between groups.

One cause of this may have been the reverse pattern in lateral enamel formation time occurring between the molar and canine groups, where instead the IGD-present canines had formation times roughly 6 months slower than the IGD-absent canines. This suggests that the IGD-present canines formed faster overall with the potential for inter-tooth variation being more notable than that which can be observed from DSRs alone. Another possibility is that the outer regions of lateral enamel for all tooth types and IGD groups were forming after the 6-18 month period where all IGD observed here had formed. This could suggest that any difference in the inter-group variation of the outer DSRs was the result of levelling vitamin D levels and thereby a return to unaffected enamel formation patterns.

DSR distribution between and within groups

While the comparisons of the equivalent enamel region mean DSRs between the two groups was unclear in places, a review of the variation within each group and region by way of the distribution of growth rates may further illuminate the potential impact of vitamin D deficiency on concurring enamel growth. For all lateral enamel regions, DSRs were found to vary in their distribution significantly more in the IGD-present group than in the IGD-absent group. Similar, if not statistically tested variations, have been observed in past research. For instance, in a recent case where all published human DSR data (at time of publishing) was collated for regions of lateral and cuspal enamel, SD variation was observed to typically lie around <0.30µm/day, with outliers normally <0.40µm/day (see Table 5 in Aris et al., 2020b). Moreover, this DSR data and that which has been subsequently published, appears to show the most common regions to present high SD are the inner and outer regions, but with minimal fluctuations within individual populations (Aris et al., 2020a, 2020b). In regards to inner and outer regions of enamel, our findings follow this trend, with the most marked differences in DSR distribution occurring in these regions between the IGD-present and IGD-absent groups (Table 1). What is new, however, is that these identified variations come from within a single population suggesting that the presence of IGD, and therefore vitamin D deficiency, correlates with a wider distribution and less consistent pattern of enamel growth.

To further contextualise the levels of distribution seen here, the SD levels of the IGD-present group, while particularly high by the standards outlined previously, are not unheard of. While examples of this level of variation are rare, they can be seen in analysis of British Roman teeth (Aris et al., 2020b) and modern South African teeth (Lacruz and Bromage, 2006). However, in both these cases the SD was high across all regions of the given population; whereas here, while the IGD-present group was significantly more variable than the IGD-absent group in all regions, the individual SD values for the mid and inner regions were within expected ranges for human populations (see Table 5 of Aris et al., 2020b). Our data are therefore unique with the IGD-present group showing SD on the expected scale for the inner and mid region, but exceptionally high in the outer region, while still significantly varying from the IGD-absent group of the same population.

These observations potentially explain the inconsistencies within the analysis of equivalent mean DSRs between the groups. This expanded analysis therefore suggests that vitamin D deficiency (identified via IGD) does not necessarily cause an increase in mean DSRs (as inner and mid test results indicate), but rather it results in an interruption in secretion of enamel matrix, subsequently causing inconsistent developmental rates across the enamel cap. Future research would benefit from replicating the analysis here on cervical and cuspal DSRs on a larger sample to further investigate this. This would also help explore the idea that the impact of vitamin D deficiency on enamel growth is localised (similar to how it is in enamel), influencing the variability in enamel growth and formation rates for regions forming at the same time as IGD. Future research is therefore also encouraged to analyse dental samples with more extensive evidence of multiple IGD formations.

Potential differences between tooth types

Typically, analyses such as those presented here investigate individual tooth types such as molars (e.g., Aris et al., 2020b; Beynon, Dean, and Reid, 1991; Lacruz and Bromage, 2006; Mahoney, 2008; Smith et al., 2007) or anterior teeth (canines and incisors; Aris et al., 2020a; Aris and Street, 2021; Birch and Dean, 2009; FitzGerald, 1998; FitzGerald and Hillson, 2009; Reid, Beynon, and Ramirez Rozzi, 1998a; Schwartz et al., 2001). In some cases teeth have been pooled within these categories, but it is unusual to pool teeth from between these groups as has been done here. There is also only one case where DSRs are not compared between groups through a grand mean (Aris and Street, 2021). It is possible therefore that the DSR variations and high distribution between the IGD-present and IGD-absent groups could be the result of this pooling of tooth types, and/or taking six DSR measures for each region of each tooth. However, comparison of tooth-type specific groups show relatively small differences between the relative IGD groups (see Table 3), and all tooth types analysed here were relatively equal in their representation of each group analysed, and for each enamel region analysed. As a result, any impact of pooling growth data collected from different teeth would have been consistent in both groups. Therefore, we do not expect that pooling growth data for different teeth has any negative impact on the conclusions drawn here. However, the enamel formation calculations suggest some variation in that data between the canines and molars, and thus future research is recommended to analyse tooth types separately when factoring in enamel thickness to confirm the previous suggestion.

The impact of Vitamin D deficiency on daily secretion rates

In seeking to explore the potential relationship between the occurrence of IGD and the variable DSRs observed in the study sample, further consideration was given to vitamin D's role in cellular activity. As noted previously, vitamin D plays a significant role in gene expression through its relationship with vitamin D receptors (VDR) in the target cells. Two calcium-binding proteins whose expression is regulated by the presence of Vitamin D are Calbindin-D28k and Calbindin-D9k. They have been identified in numerous tissues including those of the kidney, placenta, and cartilage (Onisihi et al., 2008: 117). Of the two proteins, Calbindin-D9k is most closely regulated by Vitamin D and directly associated with vitamin-D dependent calcium homeostasis (Onishi et al., 2008: 122). Indeed, Calbindin-D9k is directly involved in the mineralisation of tissues; for example, in bone, it is present in both osteoblasts and osteoclasts. Moreover, Bailleul-Forestier et al. (1996) demonstrated that vitamin D plays a significant role in regulating odontogenesis from the very earliest stages of tooth formation through to mineralisation. The reason being that both Calbindin-D28k and Calbindin-D9k are present in teeth, where they serve different purposes. Onishi et al. (2008) found that Calbindin-D9K was localised in the maturation ameloblasts where the active transportation of calcium was required. In contrast, Calbindin-D28K was expressed by secretory ameloblasts, and was not involved in the vitamin-D dependent calcium transport that occurs during enamel maturation.

Through their investigation of IGD in rodent molars, Kagayama et al. (1997) found a strong correlation between IGD and the early stages of dentine formation. It was found that IGD formation was not associated with the secretory stage of amelogenesis but, rather, with the maturation stage of enamel formation. They suggest that the interaction between the epithelial-mesenchymal cells during the later stages of tooth formation is fundamental in determining whether or not interglobular dentine appears; Onishi et al. (2008) later showed that this process was associated with the vitamin-D regulated expression of Calbindin-D9K. If vitamin D deficiency has such an impact on Calbindin-D9K and the disruption of calcium homeostasis during the maturation stage of enamel formation then it seems possible that it could also disrupt the mineralisation of the tooth enamel to such an extent that we have seen variable lateral enamel DSRs in those individuals who exhibited IGD in our study sample.

Conclusions

The presence of IGD correlates with variable lateral enamel DSRs, particularly with an increase in distribution of regional growth rates between IGD-present and IGD-absent groups within the same population - with most notable variations occurring when enamel was forming at the same time as IGD. While it should be noted that DSRs here relate to the rate of more organic enamel matrix (as opposed to enamel mineralisation during the amelogenesis maturation stage), this evidence strongly suggests that the interruption of vitamin D deficiency on the development of dentine also impacts the development of enamel, potentially in a similarly time-period-localised manner. This highlights the value of conducting histological research on populations and individuals with identifiable pathologies and/or nutritional deficiencies in order to expand our knowledge on the plasticity of enamel growth in early life.

References

Antoine, D. (2001). *Evaluating the periodicity of incremental structures in dental enamel as a means of studying growth in children from past human populations*. University of London, University College London (United Kingdom).

Antoine, D., Hillson, S., & Dean, M. C. (2009). The developmental clock of dental enamel: a test for the periodicity of prism cross-striations in modern humans and an evaluation of the most likely sources of error in histological studies of this kind. *Journal of Anatomy*, 214(1), 45-55.

Aris, C. (2020). The histological paradox: methodology and efficacy of dental sectioning. *Papers from the Institute of Archaeology*, 29(1), 1-16.

Aris, C. (2022). A contextualised enamel growth rate and thickness data set collected from British populations spanning the past 2000 years. *Dental Anthropology*, 35(1), 3-15.

Aris, C., Mahoney, P., & Deter, C. (2020a). Enamel growth rates of anterior teeth in males and females from modern and ancient British populations. *American Journal of Physical Anthropology*, 173(2), 236-249.

Aris, C., Mahoney, P., O'Hara, M. C., & Deter, C. (2020b). Enamel thickness and growth rates in modern human permanent first molars over a 2000 year period in Britain. *American Journal of Physical Anthropology*, 173(1), 141-157.

Aris, C., & Street, E. (2021). Growth rates of accessory human enamel: a histological case study of a modern-day incisor from Northern England. *Dental Anthropology Journal*, 34(1), 3-12.

Bailleul-Forestier, I., Davideau, J., Papagerakis, P. *et al.* (1996) Immunolocalization of Vitamin D Receptor and Calbindin-D28k in Human Tooth Germ. *Pediatric Research*, 39(4), 636–642.

Berdal, A., Papagerakis, P., Hotton D, Bailleul-Forestier, I., Davideau, J.L. (1995). Ameloblasts and odontoblasts, target-cells for 1,25-dihydroxyvitamin D3: a review. *International Journal of Developmental Biology*, 39(1), 257–262.

Berkovitz, B. K., Holland, G. R., & Moxham, B. J. (2002). Enamel. *Oral Anatomy, Histology and Embryology, 3rd edition*, (pp. 110-111). London: Mosby Publishing.

Beynon, A. D., Clayton, C. B., Ramirez Rozzi, F. V. R., & Reid, D. J. (1998). Radiographic and histological methodologies in estimating the chronology of crown development in modern humans and great apes: a review, with some applications for studies on juvenile hominids. *Journal of Human Evolution*, 35(4), 351-370.

Beynon, A. D., Dean, M. C., & Reid, D. J. (1991). Histological study on the chronology of the developing dentition in gorilla and orangutan. *American Journal of Physical Anthropology*, 86(2), 189-203.

Birch, W., & Dean, C. (2009). Rates of enamel formation in human deciduous teeth. In T. Koppe, G. Meyer, K. W. Alt, A. Brook, M. C. Dean, I. Kjaer, & M. F. Teaford. *Comparative dental morphology*. Vol. 13 (pp. 116-120). Karger Publishers.

Birch, W., & Dean, M. C. (2014). A method of calculating human deciduous crown formation times and of estimating the chronological ages of stressful events occurring during deciduous enamel formation. *Journal of Forensic and Legal Medicine*, 22(1), 127-144.

Botelho, J., Machado, V., Proença, L., Delgado, A. S. & Mendes, J. J. (2020) Vitamin D Deficiency and Oral Health: A Comprehensive Review. *Nutrients*, 12(5), 1471

Boyde, A. (1963). Estimation of age at death of young human skeletal remains from incremental lines in the dental enamel. In *Third International Meeting in Forensic Immunology, Medicine, Pathology and Toxicology.* Vol. 1 (pp. 36-37). Plenary session 11A.

Boyde, A. (1989). In *Teeth* (pp. 309-473). Berlin: Springer-Verlag.

Boyde, A. (1990). Developmental interpretations of dental microstructure. In *Primate Life History and Evolution*, (pp. 229-267). New York: Wiley-Liss.

Brickley, M., & McKinley, J. (2004). Guidance to standards for recording human skeletal remains. IFA Technical Paper 7. IFA.

Brickley, M., & Ives, R. (2008). *The Bioarchaeology of Metabolic Bone Disease*. Oxford: Academic Press.

Brickley, B.B., Moffat, T. & Watamaniuk, L. (2014). Biocultural Perspectives of Vitamin D Deficiency in the Past. *Journal of Anthropological Archaeology*, 36(1), 48–59.

Brickley, M. B., & Mays, S. (2019). Metabolic Disease. In J. E. Buikstra, *Identification of Pathological Conditions in Human Skeletal Remains*. Vol 1. (pp. 531–566). Cambridge, MA: Academic Press.

D'Ortenzio, L., Ribot, I., Raguin, E., Schattmann, A., Bertrand, B., Kahlon, B., & Brickley, M. (2016). The rachitic tooth: A histological examination. *Journal of Archaeological Science*, 74 (1), 152-163.

Dean, M. C. (1995). The nature and periodicity of incremental lines in primate dentine and their relationship to periradicular bands in OH 16 (Homo habilis). In *Aspects of dental biology: Paleontology, anthropology and evolution*. Vol 1. (pp. 239-265).

Dean, M. C. (1998). A comparative study of cross striation spacings in cuspal enamel and of four methods of estimating the time taken to grow molar cuspal enamel in *Pan*, *Pongo* and *Homo*. *Journal of Human Evolution*, 35(4), 449-462.

Dean, M. C., Beynon, A. D., Reid, D. J., & Whittaker, D. K. (1993). A longitudinal study of tooth growth in a single individual based on long-and short-period incremental markings in dentine and enamel. *International Journal of Osteoarchaeology*, 3(4), 249-264.

Dowd, D. R., & MacDonald, P. N. (2013). Vitamin D Receptor. In W.J. Lennarz & M. D. Lane (eds). *Encyclopaedia of Biological Chemistry, Second Edition*. Vol 1. (pp. 540-544). London: Academic Press.

FitzGerald, C. M. (1998). Do enamel microstructures have regular time dependency? Conclusions from the literature and a large-scale study. *Journal of Human Evolution*, 35(4-5), 371-386.

FitzGerald, C., & Hillson, S. (2009). Deciduous tooth growth in an ancient Greek infant cemetery. *Frontiers of Oral Biology*, 13, 178-183.

FitzGerald, C. M., & Saunders, S. R. (2005). Test of histological methods of determining chronology of accentuated striae in deciduous teeth. *American Journal of Physical Anthropology*, 127 (3), 277-290.

Goodman, A. H., & Song, R. J. (1999). Ages at formation of linear enamel hypoplasias. *Human Growth in the Past: Studies from Bones and Teeth*, 135(3), 210.

Guatelli-Steinberg, D., & Lukacs, J. R. (1999). Interpreting sex differences in enamel hypoplasia in human and non-human primates: Developmental, environmental, and cultural considerations. *American Journal of Physical Anthropology*, 110(S29), 73-126.

Hemer, K. A., & Verlinden, P. (2020). Vitamin D Deficiency Rickets In Early Medieval Wales: A Multi-Methodological Case Study. *Childhood in the Past*, *13*(1), 20-37.

Hillson, S. (1996). *Dental Anthropology*, (pp. 118-147). Cambridge: Cambridge University Press.

Holick, M. F. (2007). Vitamin D Deficiency. *The New England Journal of Medicine*, 357(1), 266–281.

Holt, S. A., Reid, D. J., & Guatelli-Steinberg, D. (2012). Brief communication: premolar enamel formation: completion of figures for ageing LEH defects in permanent dentition. *Dental Anthropology Journal*, 25(1), 4-7.

Jayawardena, C., Nandasena, T., Abeywardena, A., & Nanayakkara, D. (2009). Regional distribution of interglobular dentine in human teeth. *Archives of Oral Biology*, 54(11), 1016-1021.

Kagayama, M., Zhu, J. X, Sasano, Y., Sato, H., & Mayanagi, H. (1997) Development of interglobular dentine in rat molars and its relation to maturation of enamel. *Anatomy and Embryology (Berl)*, 196(6): 477-83

Kajiyama, S. (1965). Total number of regular incremental lines in the enamel of human permanent teeth. *Nihon University Dental Journal*, 39 (1), 77-83.

Kalpana, R., & Thubashini, M. (2015) Talon Cusp: A Case Report and Literature Review. *Oral and Maxillofacial Pathology Journal*, 6(1): 594-596

Keller, H., & Wahli, W. (1997). Steroid Hormone and Related Receptors. In E. Bitter & N. Bitter (Eds). *Principles of Medical Biology*. Vol 10 (pp. 255-296). London: Elsevier.

Kongsbak, M., Levring, T.B., Geisler, C. von Essen, M.R. (2013). The vitamin D receptor and T cell function. *Frontiers in Immunology*, 4(1), 1–10.

Kuhn, L.T. (2001). Bone Mineralization. In K. H. Jürgen Buschow, R. W. Cahn, M. C. Flemings, B. Ilschner, E. J. Kramer, S. Mahajan, & P. Veyssière (Eds.) *Encyclopedia of Materials: Science and Technology*. Vol 1. (pp. 787-794). London: Elsevier.

Lacruz, R. S., & Bromage, T. G. (2006). Appositional enamel growth in molars of South African fossil hominids. *Journal of Anatomy*, 209(1), 13-20.

Lukacs J. R. (1989). Dental paleopathology: methods for reconstructing dietary patterns in prehistory. In M. Y. Iscan & K. A. R. Kennedy (Eds). *Reconstruction of Life from the Skeleton*. Vol 1. (pp. 261-286). New York: Liss.

Lukacs, J. R. (1991). Localized enamel hypoplasia of human deciduous canine teeth: prevalence and pattern of expression in rural Pakistan. *Human Biology*, 63(4), 513-522.

Lukacs, J. R. (1992). Dental paleopathology and agricultural intensification in South Asia: new evidence from Bronze Age Harappa. *American Journal of Physical Anthropology*, 87(2), 133-150.

Lukacs, J. R. (1999). Enamel hypoplasia in deciduous teeth of great apes: Do differences in defect prevalence imply differential levels of physiological stress?. *American Journal of Physical Anthropology*, 110(3), 351-363.

Lukacs, J. R., & Joshi, M. R. (1992). Enamel hypoplasia prevalence in three ethnic groups of northwest India: A test of daughter neglect and a framework for the past. *Journal of Paleopathology*, 2(1), 359-372.

Lukacs, J. R., & Pal, J. N. (1993). Mesolithic subsistence in North India: inferences from dental attributes. *Current Anthropology*, 34(5), 745-765.

Lukacs, J. R., & Walimbe, S. R. (1998). Physiological stress in prehistoric India: new data on localized hypoplasia of primary canines linked to climate and subsistence change. *Journal of Archaeological Science*, 25(6), 571-585.

Lukacs, J. R., & Guatelli-Steinberg, D. (1994). Daughter neglect in India: LEH prevalence and the question of female biological superiority. *American Journal of Physical Anthropology*, 18(1), 132.

Mahoney, P. (2008). Intraspecific variation in M1 enamel development in modern humans: implications for human evolution. *Journal of Human Evolution*, 55(1), 131-147.

Mahoney, P. (2011). Human deciduous mandibular molar incremental enamel development. *American Journal of Physical Anthropology*, 144 (2), 204-214.

Massler, M., & Schour, I. (1946). Growth of the child and the calcification pattern of the teeth. *American Journal of Orthodontics and Oral Surgery*, 32(9), 495-517.

Mays, S., Ives, R., & Brickley, M. (2009). The effects of socioeconomic status on endochondral and appositional bone growth, and acquisition of cortical bone in children from 19th century Birmingham, England. *American Journal of Physical Anthropology*, 140(3), 410-416.

Mitchell, P. D., & Brickley, M. (Eds). 2017. Updated Guidelines to the Standards for Recording Human Remains. Chartered Institute for Archaeologists, Reading.

Mohan R. P. S., Verma, S., Singh, U., Agarwal, N., Ghanta, S., & Tyagi, K. (2013). Talon cusp in primary dentition: A case report. *International Journal of Case Reports and Images,* 4(12), 709-713.

Nanci, A., & Smith, C. E. (1992). Development and calcification of enamel. In Bonucci E. (Ed.), *Calcification in Biological Systems, 1st Edition*, (pp. 313-343). Boca Raton, FL: CRC Press.

Nanci, A., & Smith, C. E. (2020). Development and calcification of enamel. In Bonucci E. (Ed.), *Calcification in Biological Systems, 1st Edition,* (pp. 313-343). Boca Raton, FL: CRC Press. Retrieved from: https:// doi.org/10.1201/9781003068396.

Nair, R., & Maseeh, A. (2012). Vitamin D: The "sunshine" vitamin. *Journal of Pharmacology & Pharmacotherapeutics*, 3(1), 118-126

Okada, M. (1943). Har tissue of animal body. *Shanghai Evening Post*, 26-31.

Onishi T., Shintani S., Wakisaka S., & Ooshima T. (2008) Relationship of vitamin D with calbindin D9k and D28k expression in ameloblasts. *Archives of Oral Biology,* 53(2), 117-23.

Opsahl Vital, S., Gaucher, C., Bardet, C., Rowe, P.S, George, A., Linglart, A., & Chaussain, C. (2012). Tooth dentin defects reflect genetic disorders affecting bone mineralization. *Bone*, 50 (4): 989-997,

Primeau, C., Arge, S. O., Boyer, C., & Lynnerup, N. (2015). A test of inter-and intra-observer error for an atlas method of combined histological data for the evaluation of enamel hypoplasia. *Journal of Archaeological Science: Reports*, 2(1), 384-388.

Rajah, J., Jubeh, J. A., Haq, A., Shalash, A., & Parsons, H. (2008). Nutritional rickets and z scores for height in the United Arab Emirates: to D or not to D? *Pediatrics International*, 50(4), 424-428.

Reid, D. J., Beynon, A. D., & Ramirez Rozzi, F. V. R. (1998). Histological reconstruction of dental development in four individuals from a medieval site in Picardie, France. *Journal of Human Evolution*, 35(4-5), 463-477.

Reid, D. J., & Dean, M. C. (2006). Variation in modern human enamel formation times. *Journal of Human Evolution*, 50(3), 329-346.

Schwartz, G. T., Mahoney, P., Godfrey, L. R., Cuozzo, F. P., Jungers, W. L., & Randria, G. F. (2005). Dental development in Megaladapis edwardsi (Primates, Lemuriformes): implications for understanding life history variation in subfossil lemurs. *Journal of Human Evolution*, 49(6), 702-721.

Schwartz, G. T., Reid, D. J., & Dean, C. (2001). Developmental aspects of sexual dimorphism in hominoid canines. *International Journal of Primatology*, 22(5), 837-860.

Smith, T. M., Martin, L. B., & Leakey, M. G. (2003). Enamel thickness, microstructure and development in Afropithecus turkanensis. *Journal of Human Evolution*, 44(3), 283-306.

Smith, C. E., & Nanci, A. (2003). Overview of morphological changes in enamel organ cells associated with major events in amelogenesis. *International Journal of Developmental Biology*, 39(1), 153-161.

Smith, T. M., Tafforeau, P., Reid, D. J., Grün, R., Eggins, S., Boutakiout, M., & Hublin, J. J. (2007). Earliest evidence of modern human life history in North African early Homo sapiens. *Proceedings of the National Academy of Sciences*, 104(15), 6128-6133.

Snoddy, A. M., Buckley, H., King, C., Kinaston, R., Nowell, G., Gröcke, D., & Petchey, P. (2020). 'Captain of all these men of death': an integrated case study of tuberculosis in nineteenth-century Otago, New Zealand. *Bioarchaeology International*, 3(4), 217-237.

Tsuchiya, M., Sasano Y., Kagayama, M., & Watanabe, M. (2002). The extent of odontoblast processes in the dentine is distinct between cusp and cervical regions during development and ageing. *Archives of Histology and Cytology*, 65(2), 179–88.

Veselka, B., Brickley, M. B., D'Ortenzio, L., Kahlon, B., Hoogland, M. L., & Waters-Rist, A. L. (2019). Micro-CT assessment of dental mineralization defects indicative of vitamin D deficiency in two 17th–19th century Dutch communities. *American Journal of Physical Anthropology*, 169(1), 122-131.

Zheng, J., Li, Y., Shi, M. Y., Zhang, Y. F., Qian, L. M., & Zhou, Z. R. (2013). Microtribological behaviour of human tooth enamel and artificial hydroxyapatite. *Tribology International*, 63 (1), 177-185.

An Investigation of Enamel Hypoplasia and Weaning through Histomorphological Analysis and Bayesian Isotope Mixing Models

Panagiota Bantavanou, [1+] Elissavet Ganiatsou, [1+] Angelos Souleles, [1] Angeliki Georgiadou, [1] Panagiota Xanthopoulou, [1] Asterios Aidonis, [1] and Christina Papageorgopoulou [1*]

[1] Laboratory of Physical Anthropology, Department of History and Ethnology, Democritus University of Thrace

Keywords: dental microstructure, paleopathology, stable isotope analysis, incremental dentine, ancient Greece, dental anthropology

ABSTRACT Enamel hypoplasia (EH) is a developmental defect, frequently used in bioarchaeological research to assess the nutrition and health in infants and children. Anthropological studies suggest that EH relates to disease and malnutrition especially during weaning, a hypothesis that up to now has not been examined empirically in ancient populations.

In the present study, we reconstructed the weaning process of 66 individuals from ancient Thessaloniki (4th c. BC-16th c. AD), a metropole in southeastern Europe, to explore the effect of breast milk consumption and infant diet on the development of EH. For this, we estimated the duration of weaning using stable isotope analysis on dentinal collagen of permanent first molars and breast milk proportions using Bayesian modeling. In parallel, we determined the exact formation age and duration of EH defects on the canines or the incisors of the same individuals using histomorphological analysis.

The combined results of our analyses show that individuals consuming less than 50% of breast milk during weaning, developed multiple EH defects (between 2.0-5.0 years), mostly formed close to the age of weaning or later. Our results are consistent with similar studies and provide new insights into the living conditions of children in pre-industrial and pre-vaccination contexts.

Enamel hypoplasia (EH) is a developmental defect caused by metabolic and physiological stress that affects the formation of tooth enamel (Goodman and Rose, 1990; Lewis, 2018) and is the most frequently observed pathological lesion in the dentition of ancient populations (Caufield, Li and Bromage, 2012; Hillson and Bond, 1997; Krenz-Niedbała and Kozłowski, 2013). It has been used as a standard index of health and nutritional status of infants and children in ancient societies for more than 80 years (Dąbrowski et al., 2020; Goodman, Armelagos, and Rose, 1984; Katzenberg and Herring, 1996; Sarnat & Schour, 1941).

EH is caused by the insufficient secretion of mineral and organic substances carried by ameloblasts that create the enamel layers. During tooth development, enamel is deposited daily, forming cross-striations. After 6-12 days of constant secretion, cross striations form distinct bands called Retzius lines (or perikymata) (Antoine and Hillson, 2015; Smith, 2020). Any homeostatic disruption that occurs in parallel to this process can result in insufficient secretion of enamel layers and low mineral intensity, affecting the morphology of Retzius lines that appear accentuated and malformed (known as Wilson bands) (FitzGerald, Saunders, Bondioli, and Macchiarelli, 2006; Smith, 2020).

EH is classified in four types: a) furrow, b) linear, c) pits and d) plane (Goodman and Rose, 1990;

+ These authors contributed equally
*Correspondence to:
Christina Papageorgopoulou
Laboratory of Physical Anthropology,
Department of History and Ethnology,
Democritus University of Thrace
Email: cpapage@he.duth.gr

Internationale, Fédération Dentaire, 1982). The age-at-formation of enamel defects can be estimated macroscopically based on dental growth-rate charts (Massler, Schour, and Poncher, 1941; Reid and Dean, 2000). However, the macroscopical examination of EH may lead to discrepancies in determining precisely the age-at-formation, since dental growth is affected by environmental and dietary factors (Goodman and Rose, 1990; Seow, 2017) as well as intra- and inter-population variability (Hillson and Bond, 1997; Krenz-Niedbała and Kozłowski, 2013). A far more age-specific approach that considers individual and population specific standards, is the histological examination of enamel defects (Reid and Dean, 2000). This approach enables the calculation of the enamel appositional rate and thus the precise determination of the age-at-formation and duration of each defect (Antoine, FitzGerald, and Rose, 2018; Dąbrowski et al., 2021; Martin, Guatelli-Steinberg, Sciulli, and Walker, 2008; Reid, Beynon, and Ramirez Rozzi, 1998; Reid and Dean, 2000; Risnes, 1986; Skinner and Anderson, 1991; Tagiguchi, 1966).

Despite the wide use of EH by biological anthropologists for the investigation of growth disruptions in the past, its etiology remains elusive. It has been associated with infectious diseases (e.g., yellow fever), vitamin deficiencies (A, C, D) and malnutrition (Aldred, Talacko, and Steyn, 2016; Blakey, Leslie, and Reidy, 1994; Caufield et al., 2012; Dąbrowski et al., 2020; Goodman and Armelagos, 1988; Larsen, 1987; Miszkiewicz, 2015; Roberts and Manchester, 2010; Smith, 2020). Considering that enamel hypoplasia reflects physiological and metabolic stress during early life, many researchers have linked EH to breastfeeding and weaning practices (Corruccini, Handler, and Jacobi, 1985; Dittmann and Grupe, 2000; Garland, Reitsema, Larsen, and Thomas, 2018; Goodman et al., 1984; Moggi-Cecchi, Pacciani, and Pinto-Cisternas, 1994; Sandberg, Sponheimer, Lee-Thorp, and Van Ger-

Table 1. Published studies that examine the association between enamel hypoplasia and weaning. EH: Enamel Hypoplasia, EH formation ages and weaning ages are in years.

Site	Time (AD)	N	Examination of EH	EH formation ages	Reconstruction of weaning	Weaning ages	Reference
Newton Plantation, Barbados	1660-1820	100	macroscopic examination	3.0-4.0	historical sources	2.0-3.0	(Corruccini et al., 1985)
Florence	1800-1900	83	macroscopic examination	2.0-3.0	historical sources	1.0-1.5	(Moggi-Cecchi et al., 1994)
Wenigumstadt (Aschaffenburg, southern Germany)	500-700	44	macroscopic examination	3.0	stable nitrogen isotope analysis of bone collagen	1.0-3.0	(Dittmann & Grupe, 2000)
Kulubnarti, Sudan	550-800	5	macroscopic examination	4.0-7.0	incremental dentine analysis (δ13C, δ15N)	3.0-4.0	(Sandberg et al., 2014)
Mission Santa Catalina de Guale, St. Catherine's Island, Georgia USA	1605-1680	14	histological examination	2.5-4.5	incremental dentine analysis (δ13C, δ15N)	2.5-4.5	(Garland et al., 2018)

ven, 2014) (Table 1). Indeed, weaning entails many nutritional and infectious risks for infants and is considered as an intrinsic source of physiological stress in ancient populations (Grueger and Canadian Paediatric Society, Community Paediatrics Committee, 2013; Halcrow, Miller, Pechenkina, Dong, and Fan, 2021; Katzenberg and Herring, 1996; Kendall, Millard, and Beaumont, 2021).

The study of Goodman et al. (1984), was the first to suggest the relationship between EH and weaning. However, due to methodological limitations of their time, it was not possible to acquire empirical data on weaning. Recent studies that empirically reconstructed the weaning process corroborate that poor nutrition during and after weaning causes the formation of EH (Corruccini et al., 1985; Dittmann and Grupe, 2000; Garland et al., 2018; Moggi-Cecchi et al., 1994; Sandberg et al., 2014) (Table 1). Furthermore, it has been suggested that hypoplastic defects develop some time after the completion of weaning as the immunological and nutritional benefits of breast milk are no longer provided (Cucina, 2002; Fernández-Crespo et al., 2022; Tomczyk, Tomczyk-Gruca, and Zalewska, 2012). However, it remains unclear whether the depletion of breast milk or the quality of supplementary foods instigate the formation of EH.

The precise reconstruction of the weaning process in ancient individuals has become feasible with the analysis of stable isotopes of carbon ($\delta^{13}C$) and nitrogen ($\delta^{15}N$) in dentinal collagen (Beaumont and Montgomery, 2015; Eerkens, Berget, and Bartelink, 2011). This analysis permits the accurate investigation of growth and development in ancient populations as dentinal collagen encloses dietary information during initial apposition and is hardly influenced by environmental and dietary changes thereafter (Beaumont, 2020). Experimental studies from mother-infant pairs indicate that infants during exclusive breastfeeding have elevated $\delta^{15}N$ and $\delta^{13}C$ values compared to their mothers. This difference is more evident in nitrogen (between 2-3‰) than in carbon (approximately 1‰) (Fogel, Tuross, and Owsley, 1989; Herrscher, Goude, & Metz, 2017). At the onset of weaning isotopic ratios decrease and after the complete cessation of breast milk, they stabilize and are similar to those of the adult population (Halcrow et al., 2021). These measurable shifts in isotopic ratios can be detected with the segmentation of the tooth, from crown to root into small sections (Beaumont and Montgomery, 2015; Eerkens et al., 2011). Since dentine apposition can be estimated (Dean, 2017), this analysis provides the opportunity to outline dietary changes in time-specific periods of infancy and childhood. Over the years, this temporal resolution has been increased through the optimization of the dentine sampling protocols (Beaumont nd Montgomery, 2015; Curtis, Beaumont, Elamin, Wilson, and Koon, 2022; Czermak, Fernández-Crespo, Ditchfield, and Lee-Thorp, 2020; Eerkens et al., 2011). Furthermore, the development of Bayesian isotope mixing models (Fernandes, Grootes, Nadeau, and Nehlich, 2015; Stock et al., 2018) has enabled the estimation of the relative proportions of food sources in individual diets, including the amount of breast milk consumed by infants (Chinique de Armas et al., 2022, 2017).

Leveraging Bayesian modeling, histology, and stable isotope analysis we aim to estimate the exact chronological time of appearance and duration of the EH defects, the weaning process and the infant diet, and to determine whether the duration of weaning and the amount of breast milk consumption *has an impact* on the development of enamel hypoplastic defects. The encompassing hypothesis of our study is to examine whether breast milk mitigates the risk of developing severe or recurrent forms of physiological stress during weaning that result in EH formation.

Our sample population comprises individuals from the ancient city of Thessaloniki, the capital of the Provincia Macedonia and one of the largest metropoles of the Roman Empire (Adam-Veleni, 2003). Previous stable isotope studies in the site (Ganiatsou et al., 2023; Ganiatsou, Vika, Georgiadou, Protopsalti, & Papageorgopoulou, 2022) have revealed that almost 10% of the examined individuals show evidence of physiological stress. We aim to delve deeper into this observation by examining the dentition of these individuals for hypoplastic defects. In parallel, we aim to use the Bayesian model MixSIAR on the stable nitrogen and carbon ratios (Stock et al., 2018) to estimate the relative proportion of breast milk during weaning. To the best of our knowledge, no other study has documented the breast milk proportions in relation to the formation of hypoplastic defects in archaeological populations. The present study provides novel insights into this hypothesis and utilizes advanced statistical methods to answer complex research questions about the living conditions of infants and children in ancient societies.

Materials and Methods

The archaeological site

Thessaloniki was one of the first ancient urban centers in South-eastern Europe (Figure 1) (Adam-Veleni, 2003, 2012; Karamberi, 2000, 2003; Nigdelis, 1997a; Nikakis, 2019; Vakalopoulos, 1983). Historical and archaeological evidence suggest that the foundation of Thessaloniki took place in 315/16 BC by King Cassander of Macedon who named the city after his wife, who was the sister of Alexander the Great (Adam-Veleni, 2003; Allamani-Souri, 2003; Nigdelis, 1997b). During its historical transitions from Hellenistic to Roman and then to the Byzantine period, the city grew into a multicultural, economic and political hub of the ancient world (Adam-Veleni, 2012). In 2011 during the construction of the city's Metropolitan subway, the two ancient cemeteries of the city with numerous burials were unearthed (Acheilara, 2007, 2008, 2009, 2010, 2011; Bakirtzis and Pazaras, 2006; Bakirtztis and Pazaras, 2006; Kanonidis, Lamprothanasi, and Protopsalti, 2016; Makri and Vasileiadou, 2011; Misailidou-Despotidou, 2012; Misailidou-Despotidou, Lamprothanasi, and Protopsalti, 2014; Paisidou, Vasileiadou, and Konstantinidou, 2009; Vasileiadou and Pazaras, 2010).

The sample population

The sample population dates mostly to the Roman period (1st c. BC - 4th c. AD) (Table 2). Sex and age estimations are reported in Table S1 and were performed using standard anthropological methods (Acsádi, Nemeskéri, and Balás, 1970; Brooks and Suchey, 1990; Brothwell, 1981; Buikstra and Ubelaker, 1994; Ferembach, Schwindezky, and Stoukal, 1980; Işcan, Loth, and Wright, 1984, 1985; Lovejoy, Meindl, Pryzbeck, and Mensforth, 1985; Miles, 1962; Phenice, 1969).

For the weaning reconstruction we selected 66 individuals (n=34 males, n=26 females, n=6 indeterminate), who had intact permanent molars without pathological conditions (attrition, carries). First permanent molars (M1) were selected as they develop between birth and ten years of age (AlQahtani, Hector, and Liversidge, 2010), framing a suitable time period for weaning reconstructions. Fifteen (15) molars were newly processed (see *Reconstruction of the weaning process with the Bayesian model MixSIAR*) whereas the remaining 51 have

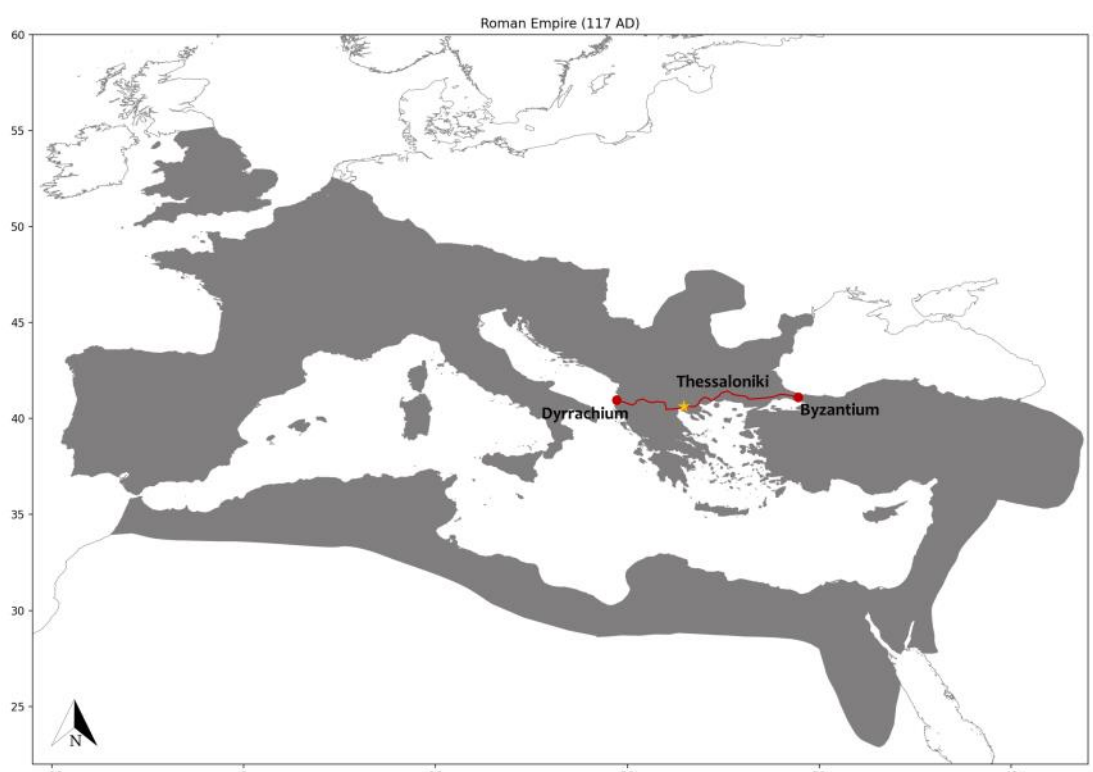

Figure 1. Extended map of the Roman Empire at 117 AD (colored in grey) showing Thessaloniki (4th c.BC- 16th c.AD). Via Egnatia (red line) connected the Adriatic (Dyrrachium) to the Black Sea (Byzantium). The map was generated in Python using the geopandas package and maps from http://awmc.unc.edu/awmc/map_data/shapefiles/political_shading/

been previously published (Ganiatsou et al., 2022; Ganiatsou et al., 2023).

Permanent canines (C) and incisors (I) from the 66 individuals were examined macroscopically for hypoplastic defects. Canines and incisors were selected as they are more susceptible to stress than premolars and molars due to their genetic canalization (Goodman and Rose, 1990; Krenz-Niedbała and Kozłowski, 2013). Furthermore, their crown forms between the first and the sixth year of life (Hillson 2014), which coincides with the period we reconstructed isotopically utilizing the molars. Twenty-seven (27) individuals with enamel hypoplasia (*n*=17 males, *n*=9 females, *n*=1 indeterminate) were identified but 26 were sampled and processed histologically, as one canine was not suitable for analysis (see *Histological examination of hypoplasia*).

Reconstruction of the weaning process with the Bayesian model MixSIAR

The weaning process was reconstructed using $\delta^{15}N$ and $\delta^{13}C$ measurements from incremental dentine collagen of first permanent molars corresponding to the life period from birth to the first six years of age. Sample preparation and collagen extraction was carried out following the Method 2 of Beaumont et al. (2015), and Brown et al. (1988), respectively and age-at-increment assignment is described in Ganiatsou et al., (2022). Weaning ages were estimated with the application WEAN, an automated tool that utilizes a computational approach to estimate the weaning duration (Ganiatsou, Souleles, and Papageorgopoulou, 2023).

The Bayesian model MixSIAR (Stock et al., 2018) was used to estimate the proportion of breast milk during weaning. This model has the advantage of allowing the incorporation of priors (e.g. fractionation factor) to account for uncertainty associated with any empirical or calculation errors (Galván, Sweeting, and Polunin, 2012; Moore & Semmens, 2008). MixSIAR necessitates three data files to provide estimates: 1) the isotopic values of consumers 2) the isotopic values of potential dietary sources and 3) the trophic discrimination factors (TDF) for each dietary source. As we are interested in the reconstruction of breastfeeding and weaning, we used the $\delta^{15}N$ and $\delta^{13}C$ values from birth until the completion of weaning. To discriminate between the weaning and the post-weaning period, we used the weaning age estimate from WEAN (Ganiatsou, Souleles, and Papageorgopoulou, 2023). In cases with no available weaning age estimate, we used the values corresponding to the first two years of life (mean weaning age estimate) (Ganiatsou, Souleles, and Papageorgopoulou, 2023). For the dietary sources' values, we used published data (breastmilk: Chinique de Armas et al., 2022, 2017, C3 and C4 plants, animal protein, freshwater fish: Dotsika et al., 2019). The trophic discrimination factors (TDFs) were taken from Ambrose (2002) and Chinique de Armas et al. (2022).

The MixSIAR model recommends that the number of dietary sources should be less or equal to the number of isotopic tracers +1 (Phillips, 2001; Schwarcz, 1991; Stock et al., 2018), i.e., in the present study $\delta^{13}C$ and $\delta^{15}N$. For this we had to reduce the number of sources to ensure the accuracy of the computational approach. To do this, we used the "isospace" function of MixSIAR to identify which dietary sources contribute to our distribution. This function plots the individual and dietary sources' isotopic values with the corrections based on the

Table 2. The number of male, female and indeterminate individuals analyzed in this study per chronological period (Hellenistic: 4th c. BC - 1st c. BC, Roman:1st c. BC - 4th c. AD, Byzantine and Post-Byzantine: 4th c. AD – 16th c. AD).

Chronological period	Males	Females	Indeterminate	Total
Hellenistic	1	4	-	5
Roman	14	15	2	31
Roman-Early Byzantine free burials*	6	1	3	10
Byzantine and post-Byzantine	13	6	1	20
Total	34	26	6	**66**

*free burials did not contain grave goods. They are dated to the Roman/ Early Byzantine period based on stratigraphy and archaeological documentation.

TDFs (Figure 2). In principle, the dietary sources should form a triangle, known as the mixing triangle (or polygon if more than three sources are included) and the consumer values should form a cluster within the mixing triangle. In both models, individual values cluster within breast milk, C3 plants and animal protein, whereas fish and C4 plants are far from the consumer values (see Figure 2). Therefore, in our analysis we selected to use as potential weaning food sources breast milk, C3 plants and animal protein and exclude the fish and C4 plants. It is important to highlight that the scope of this analysis is to examine the depletion of breast milk over time, and not to characterize diet per se. The reduction of dietary sources in our model does not exclude the possibility that some individuals had more diverse weaning diets (Ganiatsou et al., 2023; Ganiatsou et al., 2022).

After determining the number of dietary sources, two models with different breast milk values were compared to assess their validity (Chinique de Armas et al., 2022, 2017). Source data and TDFs were input as means and SDs (Table 3). Both models were run in the "short" version (chain Length=50,000, burn=25,000, thin=50, chains=3) with "Individual ID" and "age" as fixed and continuous factors respectively.

We assessed the predicted accuracy of the two models by computing the LOO (leave-one-out cross-validation) and WAIC (widely applicable information criterion), which are methods used in model selection and comparison in the field of statistics and machine learning (Risnes, 1986). LOO provides an estimate of how well the model is likely to perform on new, unseen data and WAIC quantifies the goodness of fit of a statistical model to the data, while taking into account the complexity of the model. Lower values in LOO and WAIC indicate which model has better performance (McElreath, 2020; Vehtari et al., 2017). Based on the results shown in Table 4, we selected the estimates of Model A since it has lower values than Model B, although the difference is not significant.

Histological preparation for EH age-at-formation estimation

Canines or incisors were examined histologically in order to estimate the precise age and duration of the EH defect. To achieve this, we determined the dental formation rate of appositional (cuspal) and imbricational enamel for each dental sample. This was a necessary step as there is no previous re-

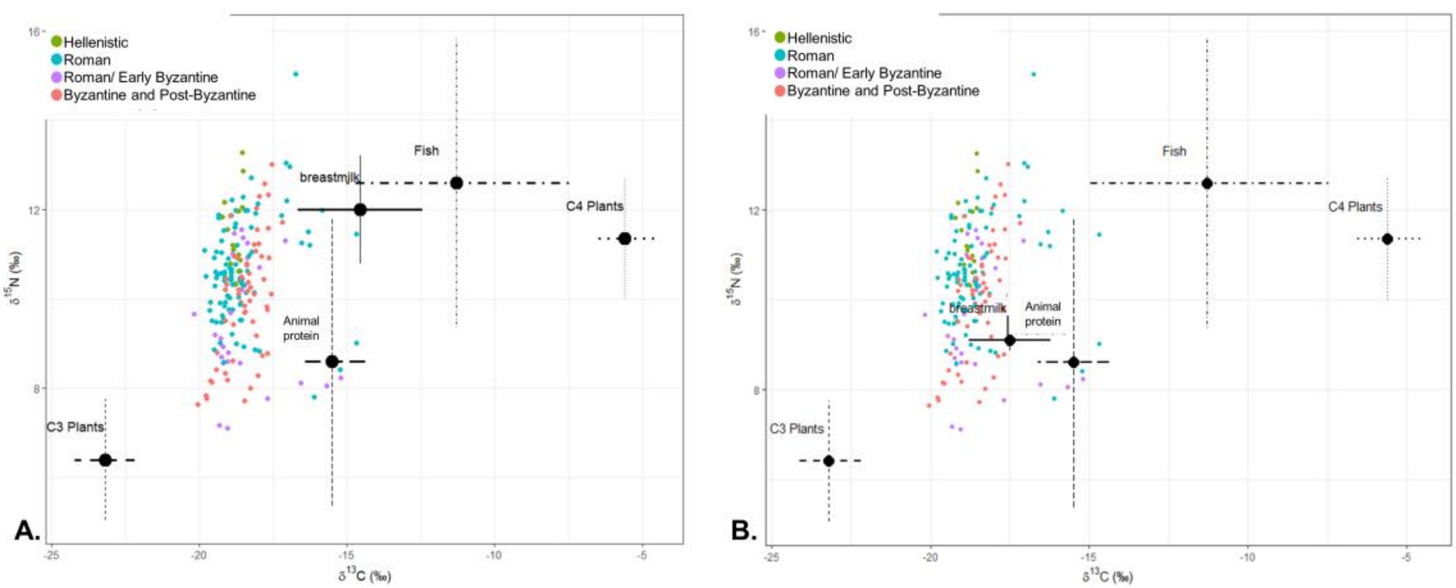

Figure 2. Isospace plots of Model A (A) and Model B (B) showing δ13C and δ15N values of individuals from ancient Thessaloniki (4th c. BC-16th c. AD) and potential dietary sources. Model A: breast milk: -19.55, 7.39, Chinique de Armas et al. 2017; C3 plants: -26.5,2.8, Dotsika et al., 2019; Animal protein: -20, 5.0, Dotsika et al., 2019). Model B: breast milk: -22.5, 5.1, Chinique de Armas et al. 2022; C3 plants: -26.5,2.8, Dotsika et al., 2019; Animal protein: -20, 5.0, Dotsika et al., 2019). Trophic discrimination factors (TDF) were taken from Chinique de Armas et al. (2022) and Ambrose (2002).

Table 3. Isotopic values and standard deviations (‰ AIR for nitrogen; VPDB for carbon) for probable dietary source components used in the MixSIAR computations for individuals from Thessaloniki (4th c. BC -16th c. AD). Source isotopic compositions and trophic discrimination factors (TDF) were taken from published literature (Ambrose, 2002; Chinique de Armas et al., 2022, 2017; Dotsika et al., 2019).

Model	Sources	Source isotopic compositions (‰) and SDs				TDF (‰) and SDs			
		$\delta^{13}C$	SD	$\delta^{15}N$	SD	$\delta^{13}C$	SD	$\delta^{15}N$	SD
A	Breastmilk	-19.55	1.1	7.39	1.19	5.5	0.7	4.4	0.1
	C3 Plants	-26.5	1.0	2.8	1.0	3.3	0.9	3.6	1.2
	Animal protein	-20	1.0	5.0	3.0	4.5	0.5	3.6	1.2
B	Breastmilk	-22.5	1.1	5.1	0.2	4.4	0.1	5.5	0.7
	C3 Plants	-26.5	1.0	2.8	1.0	3.3	0.9	3.6	1.2
	Animal protein	-20	1.0	5.0	3.0	4.5	0.5	3.6	1.2

Table 4. LOO and WAIC computations from the MixSIAR to assess the predicted accuracy of Model A and B. se_LOOic/ se_WAIC is the standard error of the two models, dLOOic/ dWAICic is the difference between each model. se_dLOOic/ se_dWAIC is the standard error of the difference between each model, weight, is an estimate of the model's probability to make the best predictions on new data, conditional on the set of models considered (McElreath, 2020; Stock et al., 2018).

Model	LOOic	se_LOOic	dLOOic	se_dLOOic	WAIC	se_WAIC	dWAIC	se_dWAIC	weight
A	168.7	32	0.0	NA	167.3	31.9	0.0	NA	0.512
B	168.8	32	0.1	0.4	167.4	31.9	0.1	0.4	0.488

search for dental formation rates in the Mediterranean populations and the acquisition of population specific data has been emphasized (Hillson and Bond, 1997; Krenz-Niedbała and Kozłowski, 2013; Ritzman, Baker, and Schwartz, 2008). Furthermore, histomorphological examination of enamel alterations caused by EH, specifically the morphological intensity of Wilson bands and the severity of enamel thinning, was conducted in order to investigate possible correlations of these micro-characteristics with the timing of the stress or sex. Prior to histological analysis, each tooth was scanned using micro-CT (SKYSCAN 1276 CMOS), to preserve the morphological characteristics for future anthropological studies.

Histological analysis of the teeth was carried out following the protocol of Hurnanen et al (2017) with minor modification. This includes: 1) rapid cleansing in accenting concentrations of ethanol (2 mins at 70% and 80% and 30 sec at 95% and 100%), 2) infiltration in xylene for 1h, 3) embedding in a two-parts epoxy resin (EpoFix, Struers). After the stabilization of the resin, the crown was separated from the root transversely, securing the root for future microscopical studies. Axial-buccolingual cross-sections of 200μm thickness were cut from the apex of the cusp to the cervix of the enamel, using a semi-automated Isomet Low Speed Shaw (Buehler) with diamond surface cutting disk (1.5mm thickness). The cross-sections were grinded, with the semi-automated grinder and polisher Labopol-20 (Struers), to 100μm, mounted on microscopic slides with mounting medium (BioMount DPX, Biognost CR) and covered with conventional coverslips. The histological analysis and observation of the enamel prisms were performed with an Axioscope A.1 (Zeiss) microscope with optical, transmitted and polarized light. The measurements of the cusp and counting of the prisms were regulated through microimages imported to Fiji software (Java 1.8.0) (Schindelin et al., 2012), captured with a digital microscope camera (AxioCam Icc3, Zeiss). In cases with minor attrition of the crown (n=6), the enamel was reconstructed in Adobe Illustrator software (CC 2015.3.1 (20.1)) and was then imported in Fiji software (Java 1.8.0_322).

To determine the formation time of cuspal enamel, we measured the enamel thickness from the dentine-enamel junction of the apex to the top point of the cusp (magnification X100) using the "Straight line" tool of Fiji software (Figure 3). The average cross-striation periodicity of enamel deposition was calculated by counting the cross-striations at 10 random locations of the cusp that were observable and countable (magnification X400). The measurement of the enamel thickness was then multiplied with the average cross-striation periodicity (Risnes, 1986) and divided by the total number of days in a year (365 days) as in formula (1).

$$Y = (X*a)/365 \quad (1)$$

Y=formation time of cuspal enamel, X=enamel thickness, a=average cross-striation periodicity

The duration of hypoplasia was determined by multiplying the sum of Retzius lines that were confined between the first and the last Wilson band, with the average cross-striation periodicity and divided by the average number of days in a month (30 days) (Figure 4). The chronological time when each hypoplastic defect began was determined by the formation time of the enamel from the cusp

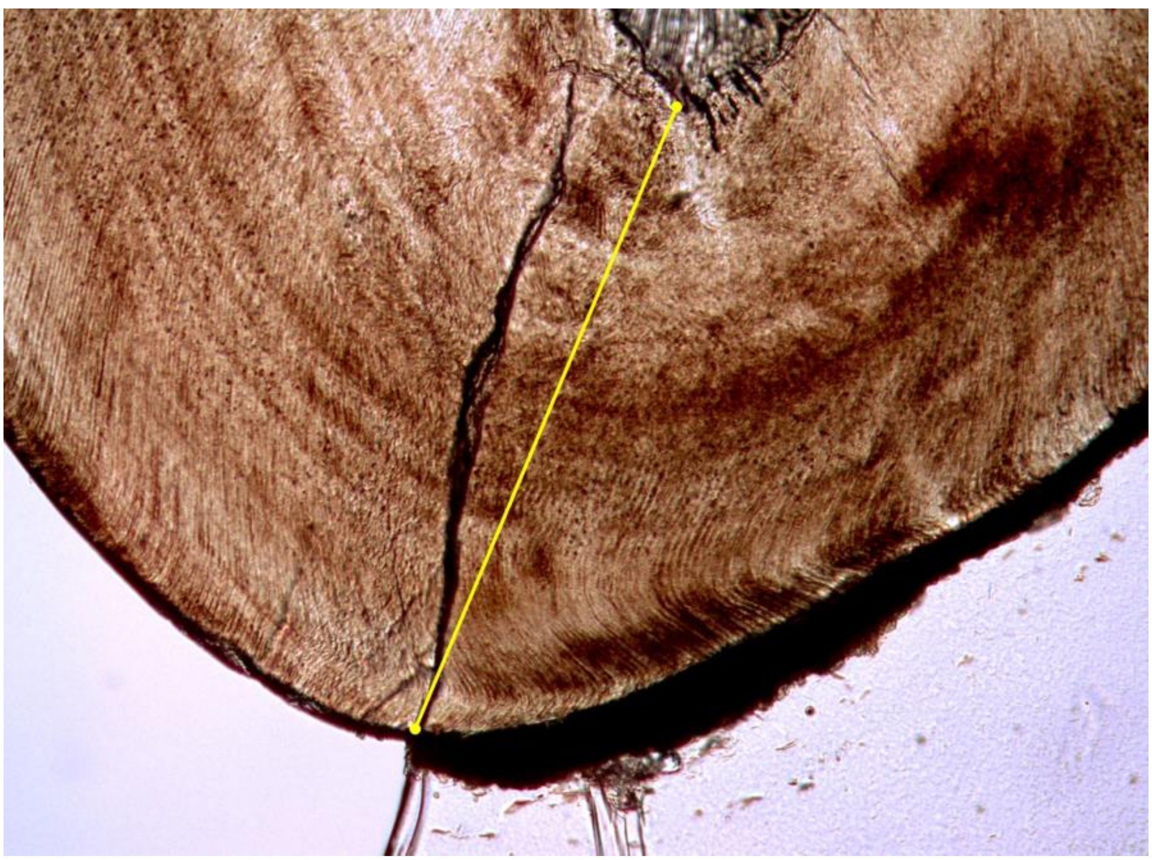

Figure 3. Microphotograph of lower canine (METi_466) of a subadult individual (4 years old) from Thessaloniki (2nd c. AD). Micro-image captured by Axiocam ICC3 (Zeiss) with magnification X100, under Axioscope A.1 (Zeiss), imported to Fiji software with the measurement of the cuspal thickness with the "Straight line" tool (yellow line).

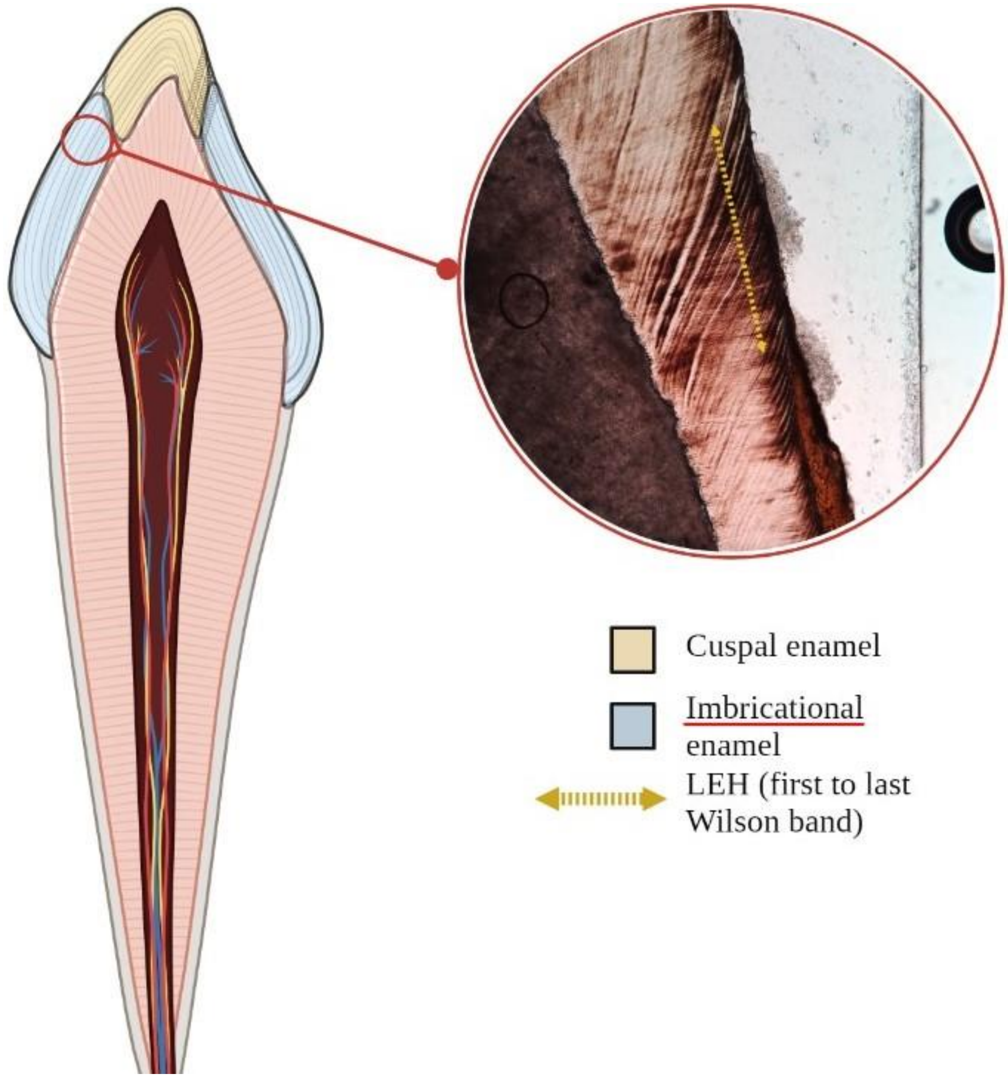

Figure 4. Canine cross-section and microimage of a LEH defect. Wilson bands are developed and demarcate the beginning and end of the LEH defect (yellow dashed arrow marking all the Wilson bands of a microphotograph of lower canine (METi_195) of a male individual (40-55 years old) from Thessaloniki (2nd c. AD Roman period)).

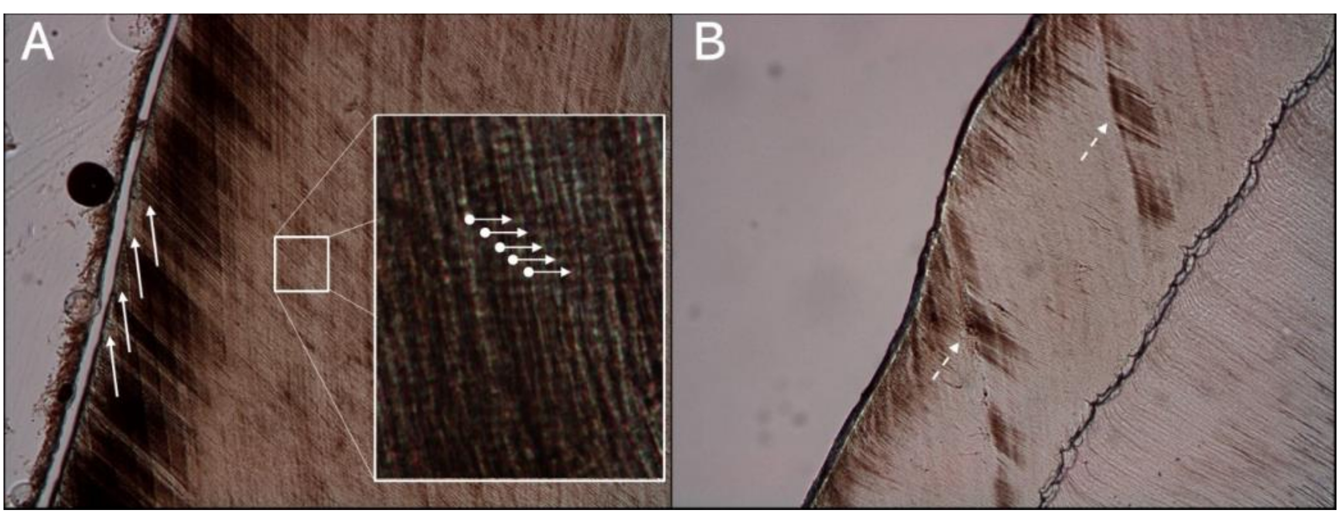

Figure 5. A. Microphotograph of lower canine (METi_199) of a young male (16-18 years) from Thessaloniki (16th c. AD). Retzius lines pointed by white arrows and cross-striations with bullet arrows on the pop-up window. B. Microphotograph of upper canine (METi_185) of a young adult male (25-30 years) from Thessaloniki (Post-Byzantine, 15-16th c AD). Wilson bands indicated with white dashed arrows. All microphotographs were captured by Axiocam ICC3 (Zeiss) with magnification X100 and X200, under Axioscope A.1 (Zeiss) optical microscope.

until the appearance of the first Wilson band (Figure 5).

In order to examine the EH episodes according to the timing of appearance we conducted descriptive analysis of the EH episodes and the chronological age of appearance. Kernel density plots were used for visualizing the concentrations and distribution of chronological ages of EH within the population and each sex group. Two-way ANOVA was performed to examine the correlation of EH defects timing between sexes after assessing the normality of the distribution with Shapiro-Wilk test.

The depth of the hypoplastic defects were examined by measuring the curvature (κ) of enamel. To calculate the curve of the EH, micro-images (magnification X100) were imported in Fiji software and run the plugin, Kappa. The plugin uses cubic B-spline curves formed by multiple 3rd degree Bézier curves. Thus, complex curvatures can be shaped with the application of a few points. Kappa plugin uses a minimization algorithm that fits the B-spline curve to the underlying data and scales them (Mary and Brouhard, 2019). Running the plugin we created open B-spline curves through point-clicking on the borders of the enamel before and through the hypoplastic defect. Calculus remnants were avoided as they do not follow the enamel shape (Figure 6). The retrieved data included the x and y coordinates of the curve and the control points (point curvature) that indicate the location and shape of the curve.

To statistically examine the curves according to the EH episodes and sex group we used area charts for visualization of the data. Considering the large size of the curve data, Kolmogorov-Smirnov test was used for normality testing instead of Shapiro-Wilk, as it is less affected by the sample size. ANOVA has three different types (Type I, Type II and Type III) to test split variations. Type III is used for data *that are unbalanced and not sequential*. Two-way ANOVA (Type III) performed for the correlation of the depth of hypoplasia through the curve data with the timing of EH episodes and sex.

The severity of the EH was examined through the color intensity of Wilson bands. "Segment line" tool of Fiji software creates a Region of Interest (ROI) of the line area that includes all the underlying data. In every EH of all teeth we *drew* segment lines on Wilson bands and retrieved data of the gray-scale color intensity and length (μm) through profile histograms of the software (Figure 7). We

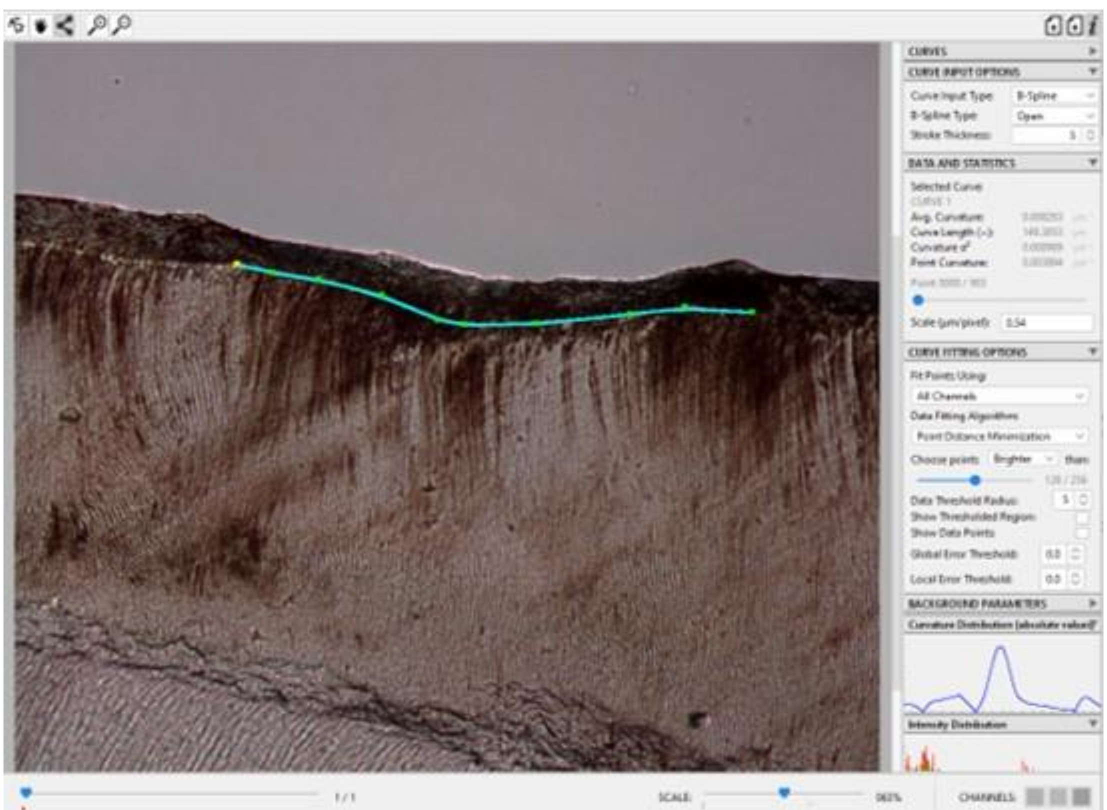

Figure 6. Micro-image of individual (METi_197) (magnification X100) of B-spline created in Fiji software using Kappa plug in.

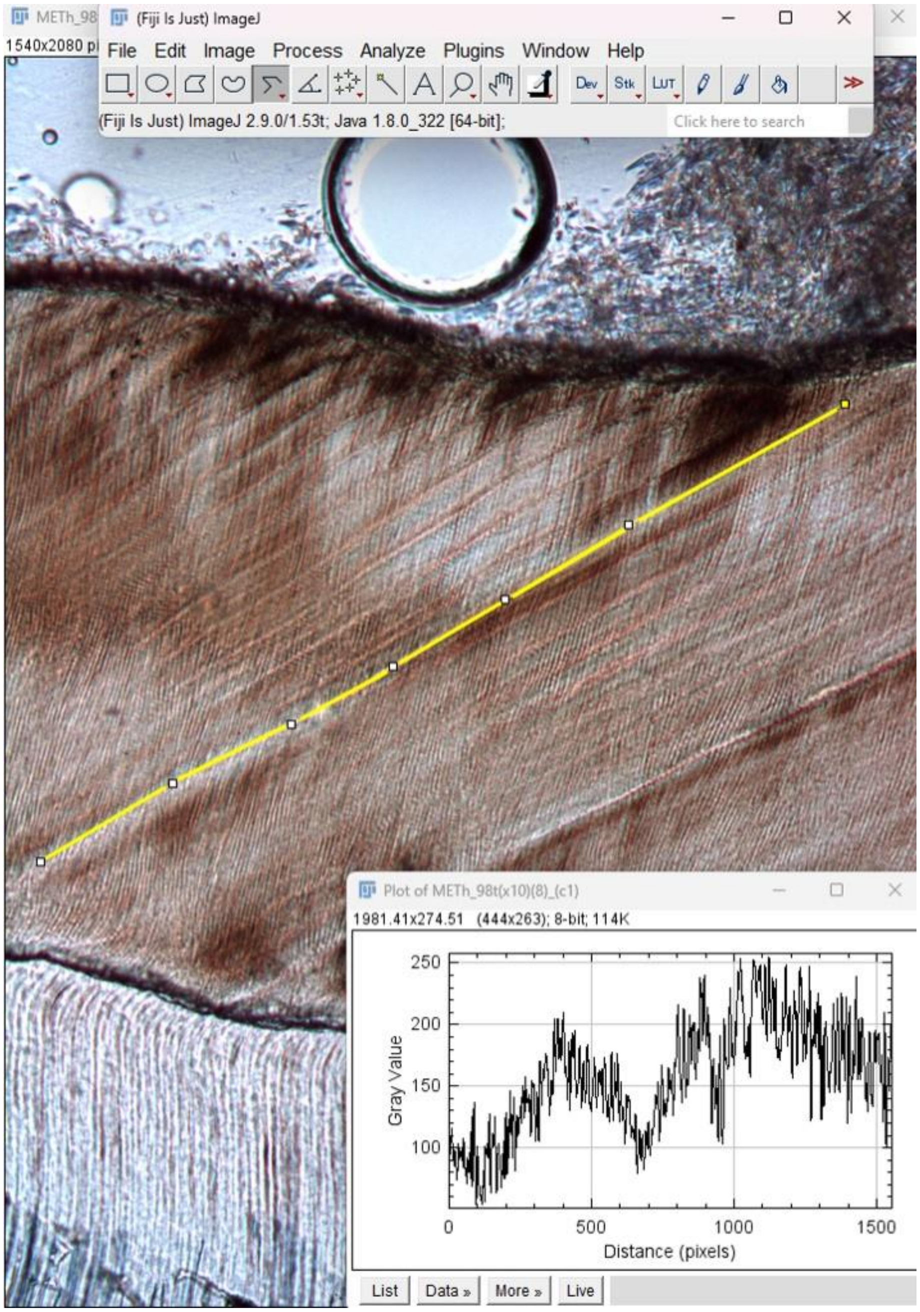

Figure 7. Micro-image of individual (METi_228) in Fiji software. Segment line tool (yellow line) marking a Wilson band, with the profile histogram showing the length of the line and the values of gray scale.

statistically examined the gray-scale color values of the Wilson bands with the EH episodes. Shapiro-Wilk test was performed for normality inspection of Wilson bands gray-scale values. Two-way ANOVA (Type III) test performed for the correlation of the gray scale intensity of Wilson bands with EH episodes.

Statistical evaluation of breast milk estimates between individuals with and without hypoplasias

The association between EH and breast milk proportion was determined by a Fisher's exact test, which is similar to a Chi-square test but more efficient in small sample sizes. Individuals were categorized into two groups based on the presence or absence of EH. In the absence of universally accepted breast milk proportions during weaning, it is not feasible to score them as "low", "medium", or "high" regarding its consumption. Therefore, to categorize breast milk proportion estimates, we used the percentiles of the distribution obtained from MixSIAR. The relationship between the breast milk proportion and the weaning duration was assessed by computing the Spearman's correlation.

Descriptive, inferential statistics and data visualization were performed in R (version 4.2.2).

Results

Reconstruction of the weaning process

A total of 225 increments were generated from the 15 newly reported individuals. Two individuals (METi_105, 109) date to the Hellenistic period, three (METi_107, 113, 466) date to the Roman period, ten (METi_133, 135, 149, 155, 173, 175, 209, 215, 231, 233,) date to the late Roman-early Byzantine period and one (METi_121) dates to the post-Byzantine period.

Out of this total, 163 were measured as we aimed to reconstruct weaning and diet during the first six years of age. Isotopic values of the 163 samples ($\delta^{15}N$ and $\delta^{13}C$) and elemental indicators (%C, %N, C: N) for collagen quality control of each sample are reported in Table S2. Overall, $\delta^{15}N$ values range between 7.06‰ and 13.68‰ (mean: 9.58‰) and of $\delta^{13}C$ range from -14.68‰ to -20.75‰ (mean: -18.43). All analyzed collagen samples (n=163) fall within the acceptable range for collagen integrity (Ambrose, 1990; DeNiro, 1985; van Klinken, 1999) (%C: 13-47%, %N: 5-17, C/ N: 2.9-3.6). The WEAN estimates of weaning completion are reported in Table S3.

The MixSIAR model estimates for potential die-

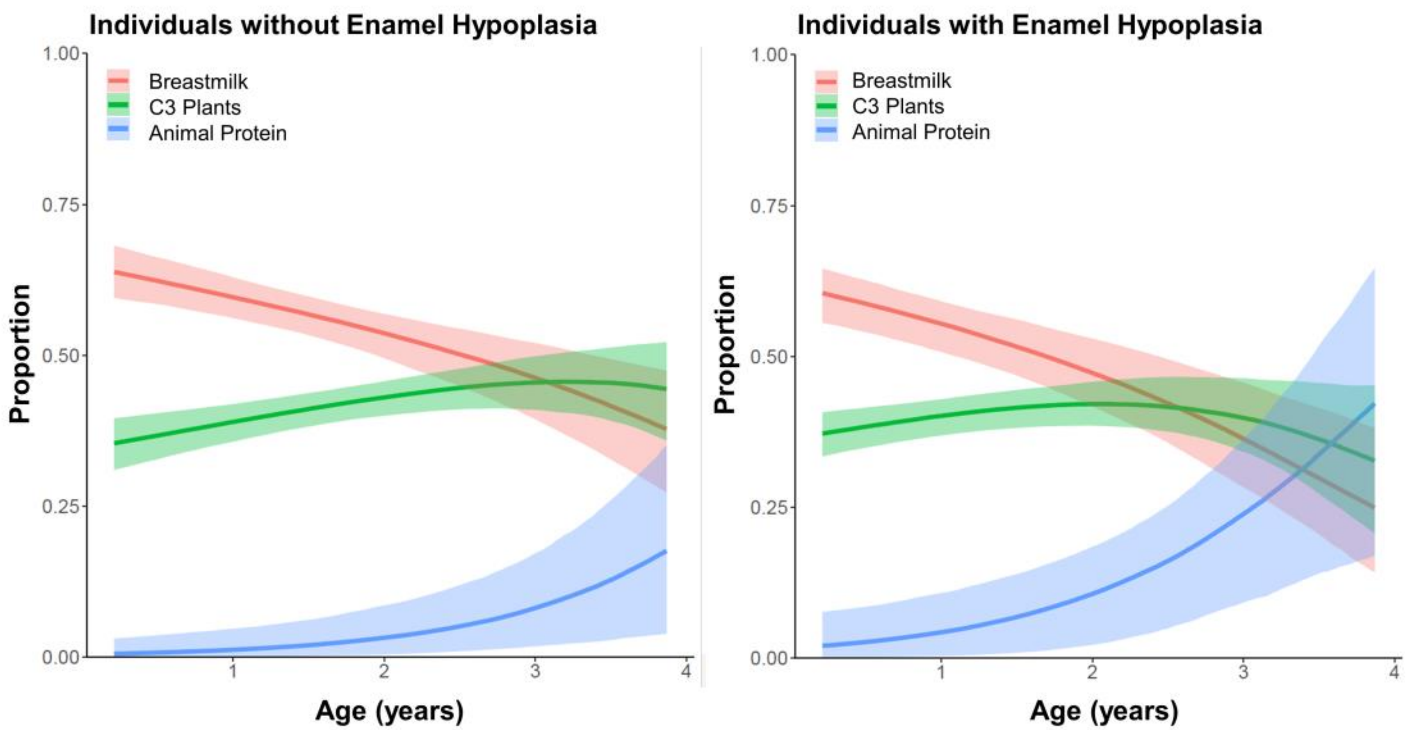

Figure 8. The proportion of breast milk, C3 plants and animal protein during the first four years of age for the individuals with and without enamel hypoplasia (EH) from ancient Thessaloniki (4th c. BC-16th c. AD) obtained from MixSIAR.

Table 5. MixSIAR model estimates depicting the probability of each dietary source during weaning for the individuals from ancient Thessaloniki (4th c. BC-16th c. AD) combining carbon and nitrogen stable isotope ratios of dentinal collagen. The percentiles serve as confidence intervals (CI) measuring this probability.

	Dietary source	5%	25%	50%	75%	95%
Individuals without hypoplasia	Breastmilk	0.48	0.52	0.54	0.57	0.60
	C3 plants	0.32	0.35	0.38	0.40	0.44
	Animal protein	0.06	0.07	0.08	0.09	0.11
Individuals with hypoplasia	Breastmilk	0.43	0.47	0.49	0.51	0.55
	C3 plants	0.31	0.34	0.36	0.38	0.42
	Animal protein	0.11	0.13	0.15	0.17	0.19

tary sources for every individual (15 newly and 51 previously analyzed) are reported in Table S4. Table 5 presents the results of the MixSIAR modelling. The provided percentiles serve as confidence intervals, showing the likelihood associated with the contribution of each dietary source into the diet. For instance, considering the breastmilk of individuals without hypoplasia, the 5th and 95th percentiles are reported as 0.48 and 0.60, respectively. To provide a more robust representation of the probability, we highlight the median at 0.54, accompanied by a 95% confidence interval ranging from 0.48 to 0.60. Individuals without EH consumed more breast milk until the cessation of weaning (54%) compared to individuals with EH (49%) (Figure 8). Individuals without EH had a diet richer in animal proteins than the ones with EH. There was no difference between the two groups on the C3 plants consumption (Table 5).

Histomorphological examination and age estimation of enamel hypoplastic defects

From the 66 individuals, 26 individuals (*n*=16 males, *n*=10 females, *n*=1 indetermined) were processed histologically. Three individuals (METi_139,201,221) date to the Hellenistic period, eleven (METi_157, 163, 189, 195, 197, 203, 223, 239, 257, 466, 71) date to the Roman period, four (METi_173, 175, 209, 231) date to the late Roman-early Byzantine period and eight (METi_121, 131, 185, 193, 199, 217, 228, 267) date to the post-Byzantine period.

One individual exhibited pitting enamel hypoplasia (PEH) (METi_231), one exhibited plane hypoplasia (METi_163), and the remaining 24 exhibited linear enamel hypoplasia (LEH). Histologically, plane hypoplasia is characterized by extensive destruction of the prismatic structure of the enamel and bending of the Wilson bands. Linear and pitting hypoplasia appear with localized thinning of the enamel and extensive number of Wilson bands (Hillson and Bond, 1997; Lukasik and Krenz-Niedbała, 2014).

Histomorphological examination of EH proved to be advantageous because it enabled the detection of defects that were not visible during the macroscopical examination. As a result, the number of hypoplastic episodes increased in 13 individuals i.e. in three individuals increased from two to three, in eight individuals from one to two and in two individuals from one to three. Furthermore, defects in two individuals (METi_199 and METi_217) that were recorded as EH by macroscopic examination were proven to be taphonomic weathering after the histological examination.

In Table 6 we present the developmental rates of cuspal and imbricational enamel. We could not estimate the cuspal enamel formation time in three individuals (METi_193, 221, 71), as the cross-striations that result in the average periodicity of enamel deposition were not observable due to taphonomic degradation. For these three individuals we used the average formation time of cuspal enamel that were generated from the same tooth type of the other individuals (Table S6). The average cross-striation periodicity emerging from the total sample of canines (upper and lower) for the population of Thessaloniki is 7.07 days. For details of the histological results see Table S6.

One individual exhibited five defects of enamel hypoplasia, six individuals three defects and 25 individuals two defects (Table S5). A young (15-21 years old) male individual (METi_163) exhibited one hypoplastic defect that was incessant for 3.9 years, appearing at the age of 2.9 years old until the age of 6.8 years old. The individual with the five defects was a subadult (6-10 years of age) (METi_466) (Table S5) who suffered five consecutive events of stress at the ages of 1.9, 2.1, 2.11, 3.7 and 4.07 years old.

For statistical analysis we grouped the episodes

Table 6. Average cross-striation periodicity of cuspal (n=23) and imbricational (n=26) enamel from the individuals of ancient Thessaloniki (4th c. BC-16th c. AD) according to tooth type (UI= Upper Incisor, UC= Upper Canine, LC= Lower Canine).

Number of teeth per tooth type	Cuspal average cross-striation periodicity (in days)	Imbricational average cross-striation periodicity (in days)
UI = 1	9.63	8.2
UC = 9	8.34	7.4
LC = 16	7.05	6.79

Table 7. Summary results of the 26 individuals from ancient Thessaloniki (4th c. BC -16th c. AD) that exhibited hypoplastic defects. Descriptive statistics of the timing of EH for each group independently.

	Values of ages		
Descriptive Statistics	**First EH**	**Second EH**	**Third EH**
Minimum	1.660	2.080	2.510
Maximum	4.500	6.160	4.670
1st Quartile	2.330	3.160	2.953
Median	2.500	3.510	3.715
Mean	2.591	3.524	3.645
3rd Quartile	2.757	3.750	4.350

of enamel hypoplasia according to the order of appearance: first, second and third EH. The fourth and fifth appearance of enamel defects were not tested as they were present only in one individual. Shapiro-Wilk test showed normal distribution (p <0.05) of the EHs values. The statistical analysis revealed two peaks of stress, at the age of 2.4 years and 3.6 years (Figure 9). The first hypoplasia occurred at the mean age of 2.5 years, and the second hypoplasia occurred at the mean age of 3.5 years. The third episode of hypoplasia does not result in a significant peak as the range is wide and the sample size (n=6) is small (Table 7). Males exhibit a peak of the first EH at the age of 2.5 years with a wide range (1.6 - 3.3 years) whereas females at the age of 2.5 years with a smaller peak at the age of 4.5 years. The differences were statistically significant (two-way ANOVA) (p <0.05). For the second hypoplastic defect, the difference between males and females was not statistically significant (p >0.05) (Figure 10). Figure S1 shows the distribution of EH episodes according sex through the historical periods.

The statistical examination of the enamel morphological alterations, namely the intensity of the Wilson bands and the thinning of the enamel created by EHs, showed different correlation patterns. Kolmogorov-Smirnov test showed normal distribution of the control point curvature values (p < 0.05). The area plots show that the first EH defects have more intense curves, with an increased thinning of the enamel whereas the hypoplastic defects that follow are progressively shallower (Figure 11). Differentiation between sexes is also apparent with the males exhibiting deeper defects than females in all first and second EH episodes (Figure 12). The other three EH episodes cannot be compared as only one male individual exhibited a third EH and only one subadult exhibited a fourth and a fifth EH defect. Two-way ANOVA showed correlation between the depth of the defects and the sex with the EHs (p < 0.05).

The intensity of Wilson bands however, examined through the gray-scale intensity, resulted no correlation with each EH defect (i.e. first, second etc). Shapiro-Wilk test showed that the data of the gray scale of Wilson bands are not normally distributed. The two-way ANOVA (Type III) showed no correlation with EH (p > 0.05).

Statistical evaluation of breast milk estimates between individuals with and without hypoplasias

The MixSIAR model estimates for the breast milk proportion did not show significant differences for the four quartiles (Table 4). Therefore, we used only the 2nd quartile (50%) and created two

Table 8. Crosstab table showing the number of individuals with and without EH who consumed less or more than 50% of breast milk during the weaning process used for Fisher's exact test (p-value: 0.02, significance level set at 0.05).

	less than 50%	**more than 50%**
Individuals with hypoplasias	15	12
Individuals without hypoplasias	6	20

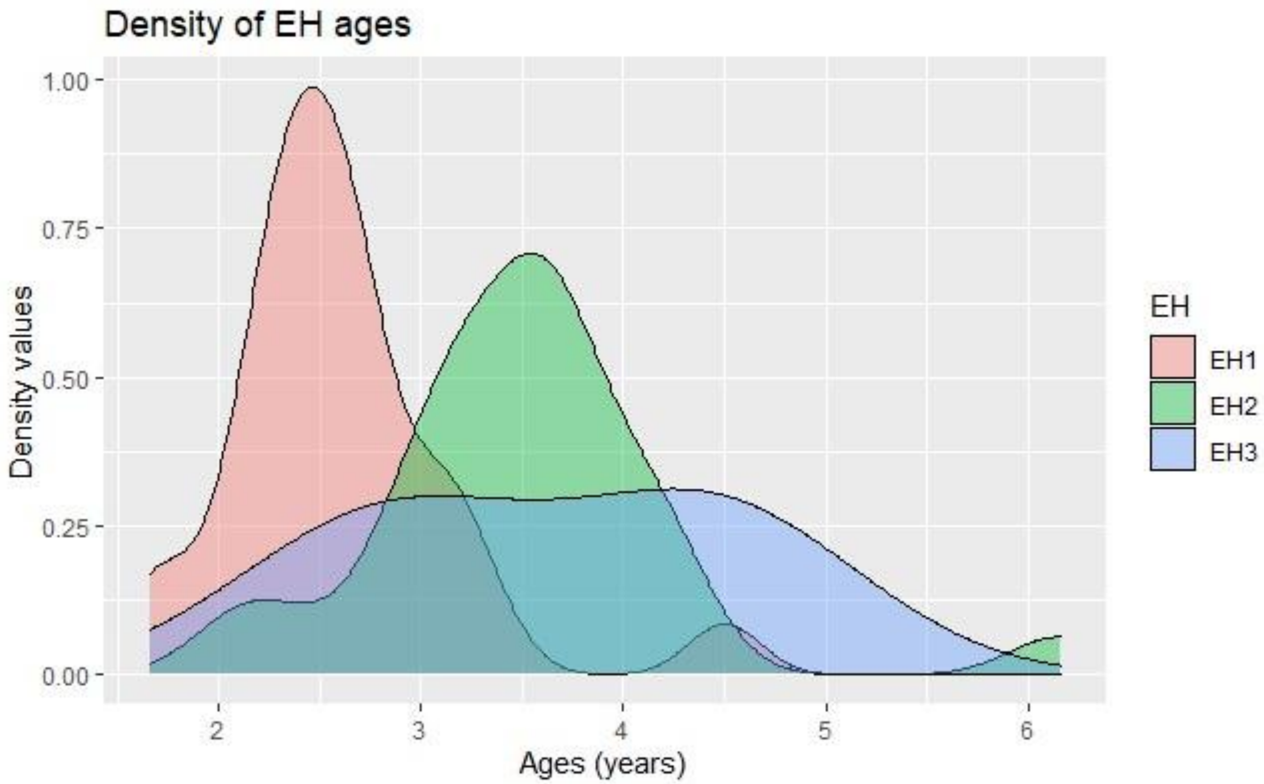

Figure 9. Kernel density plot showing the density and distribution and peaks of timing of appearance of each EH group incidences from the individuals of Thessaloniki (4th c. BC-16th c.AD). EH1 = first enamel hypoplasia, EH2= second enamel hypoplasia, EH3= third enamel hypoplasia.

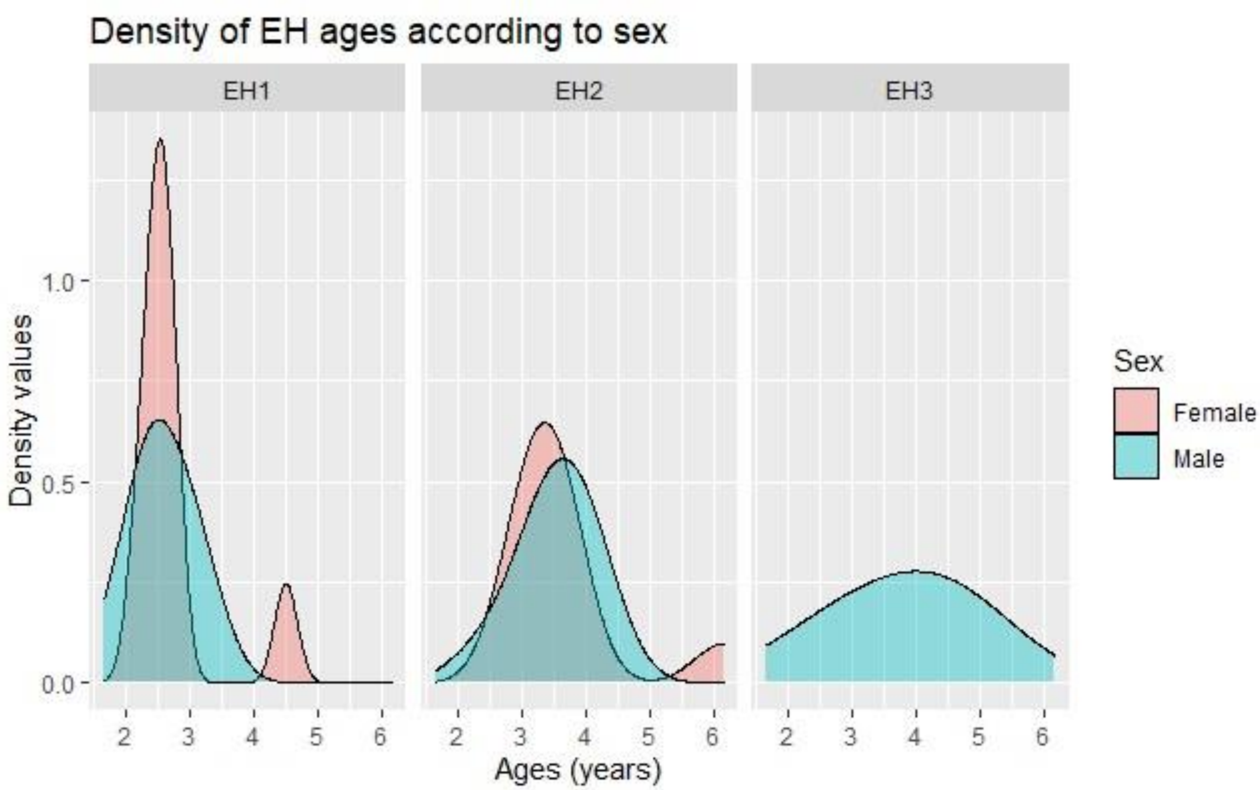

Figure 10. Kernel density plot showing the distribution and peaks of timing of appearance of each EH group incidences from the individuals of Thessaloniki (4th c. BC -16th c. AD) according to sex. Males exhibit a peak of the first EH at the age of 2.5 years with a wide age range (1.6 - 3.3 years) whereas females at the age of 2.5 years with a smaller peak at the age of 4.5 years.

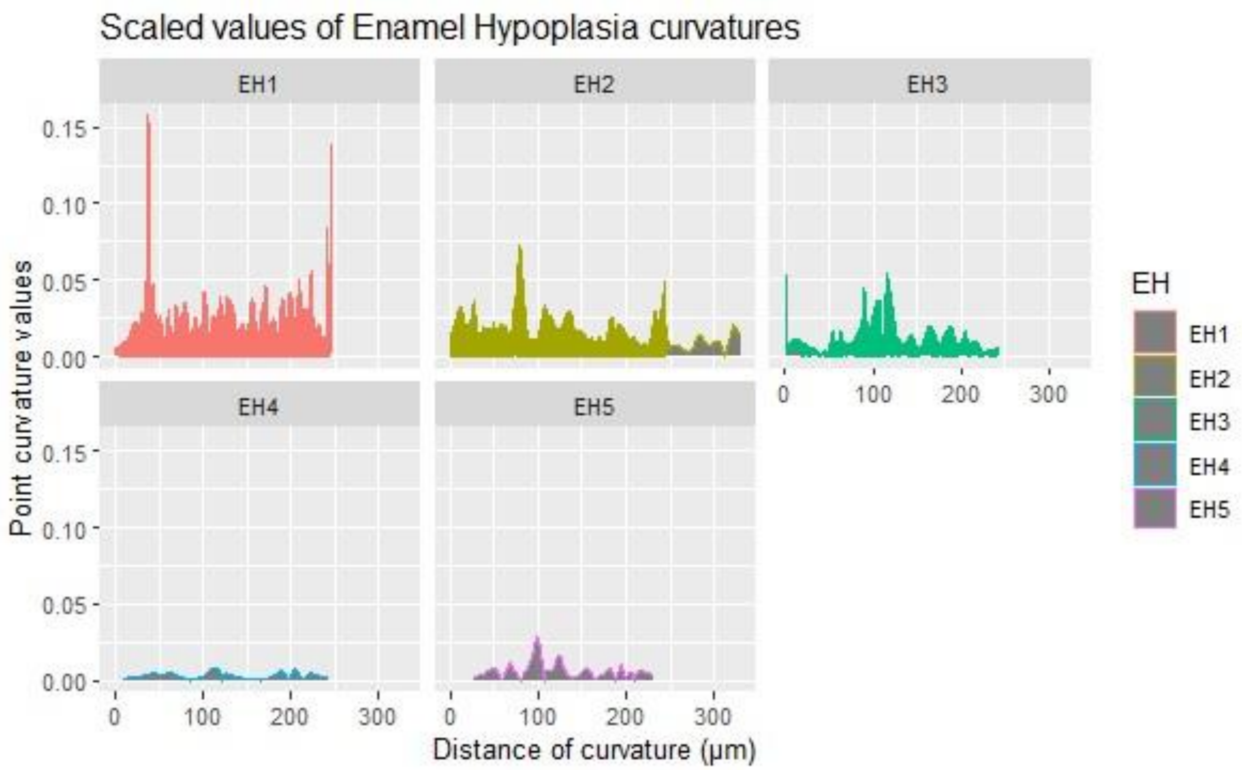

Figure 11. Area plots showing the curves of EHs from the individuals of Thessaloniki (4th c. BC -16th c. AD) according to the timing of EH. The first EH has increased points of curvature that indicate deeper defects. The second EH is less deep but are lengthier showing larger duration. The other EHs are progressively shallower.

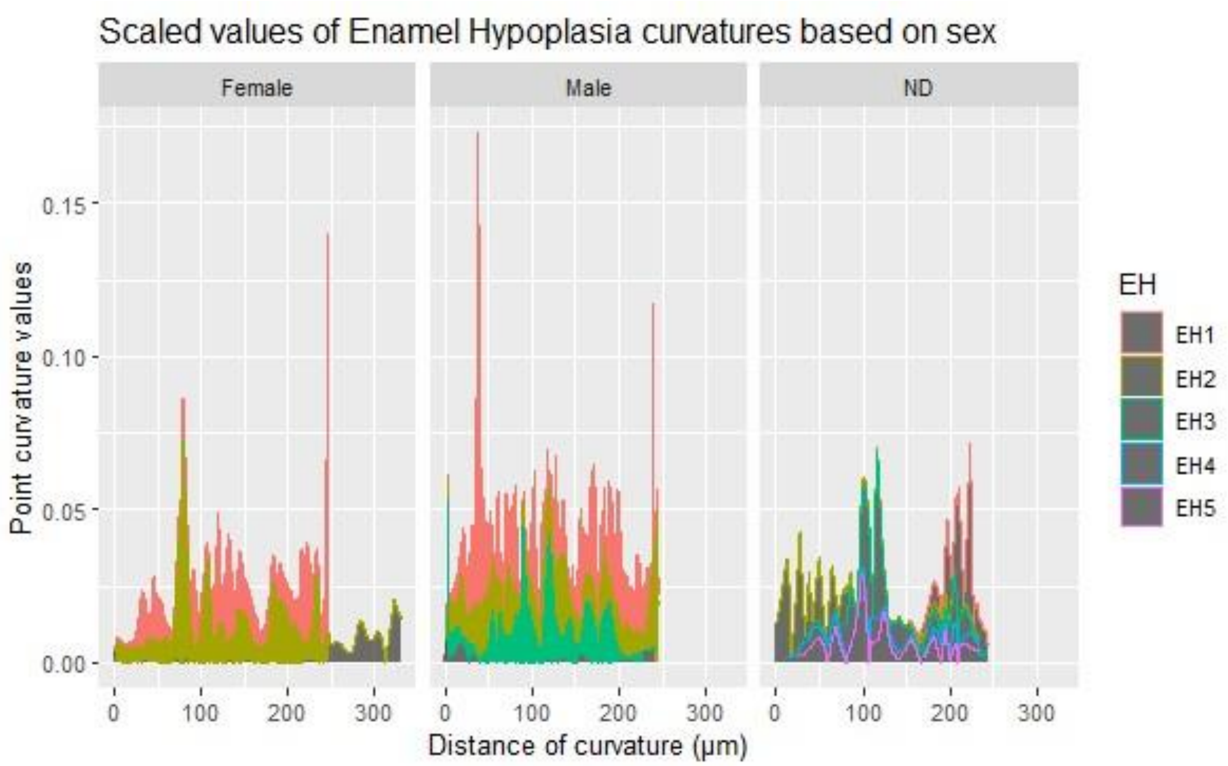

Figure 12. Area plots showing the curves of EHs from the individuals of Thessaloniki (4th c. BC -16th c. AD) according to sex. At the first and second EH males exhibited higher points of curvature than females, that indicate deeper defects.

groups: in the first, breast milk constitutes less than 50% of the total diet (“Less than 50%”), whereas in the second, breast milk constitutes more than 50% of the total diet ("More than 50%”) (Table 8). The results of Fisher's exact test showed that the difference between the two groups *is statistically significant* (p: 0.02, significance level set at 0.05). We have also found a weak positive but not statistically significant correlation between breast milk proportion and weaning age (rho = 0.040, p = 0.776). Figure S2 shows the distribution of breastmilk proportions and other food sources according to historical periods.

Discussion

The overarching question of this study was to test whether the proportion of breast milk during weaning *has an impact* on the *formation* of enamel hypoplasia. We have explored this hypothesis in 66 individuals from ancient Thessaloniki (4th c. BC-16th c. AD) by estimating: 1) the duration of weaning using incremental dentine analysis (163 newly reported increments), 2) the proportion of breast milk and other potential dietary sources during weaning using Bayesian modeling and 3) the formation ages and duration of enamel hypoplasia using histological analysis.

Enamel hypoplasia in ancient Thessaloniki

Multiple EH defects were identified in 27 out of 66 individuals (40%), formed between 2.0-5.0 years of age. All individuals developed at least two hypoplastic defects with a modal age of 2.4 years and of 3.6 years respectively, whereas six individuals exhibited a third one (Table S5). The high frequency of EH and more specifically of linear enamel hypoplasia (LEH) on Greek populations has been previously reported (Pitsios, 2012). In particular, in the study of Pitsios (2012), ancient skeletal material from five different ancient Greek cities (Leonidio, Arkadia; Tripoli, Arkadia; Markopoulo, Attica; Athens, Attica; Eretria, Euboea; Abdera, Thrace) were studied macroscopically. According to this study the frequency of LEH varied between the cities from 17% to 51% and the most affected tooth type was the upper canine. However, there is no information about differences in sex or age or more specific chronological distribution of the datasets.

In the present study, we did not identify significant differences in dental growth formation rates between males and females but found statistically significant differences in the frequency and occurrence of the first incidence of EH between the two sexes (Figure 10). In particular out of the 27 individuals that exhibited EH, the 61.5% (17/27) were males while 34.6% (9/27) were females. In females the first EH defect appears at the age of 2.2 years and does not exceed the age of 2.9 years (except for one individual), whereas males exhibit the first EH defect between the age of 1.8 and 3.4 years. Furthermore, the examination of the enamel thinning revealed that the first EH is more severe than the later and males develop more severe hypoplasias than females. These reveals a shorter and less acute stress period for females than males. This result may relate with the observation that male infants are biologically weaker than female, a phenomenon also known as the male disadvantage (Hossin, 2021). Medical studies suggest that male infants exhibit higher neonatal mortality and *more* severe morbidity compared to females (Eriksson, Kajantie, Osmond, Thornburg, and Barker, 2010; Hossin, 2021; Wong, Schreiber, Crawford, and Kumar, 2023). Alternatively, the sex difference in timing and severity of EH defects could be associated to different feeding practices as showed by previous studies (Ganiatsou et al., 2022) (Table S6). The underlying cause of this significant disparity between sexes remains unclear and is likely multifactorial. Overall, EH on a Roman-Byzantine population from Greece was a common condition indicating that in pre-vaccination and pre-industrial contexts, acute manifestations of physiological stress during childhood were frequently experienced.

Exclusive breastfeeding shapes the immune system of infants.

As infant feeding practices could be an important stress factor, we examined the breastfeeding and the weaning patterns in ancient Thessaloniki and found that the majority of EH defects (n=20/27) formed after the end of weaning and few (n=7/27) during the last phase of weaning. Similar patterns of EH formation and weaning age were found in 14 individuals from Mission Santa Catalina de Guale (1605-1680 AD) in St. Catherine's Island (Georgia, USA) and were attributed to malnutrition due to a maize-based weaning diet (Garland et al., 2018). Sandberg (2014) examined 5 individuals from the site of Kulubnarti (550-800 AD) in Sudan and suggested that morbid events resulted in the formation of EH between 4.0 and 7.0 years of age whereas, weaning was completed between 2.0-5.0 years of age according to incremental dentine analysis.

Therefore, based on the results of the present study, we suggest that breast milk consumption and EH could have a causative relationship. As we have shown, hypoplastic defects were developed in individuals consuming less than 50% of breast milk during weaning. Furthermore, in individuals with EH, the defects did not develop during the first year of life, when breast milk had constituted the major source of their nutrition (Table 8). This possibly highlights the immunological support provided by breast milk, at least during periods that is consumed in larger amounts. Breast milk is a nutritionally complete food source and is microbiologically safer compared to other foods, such as the non-pasteurized milk (Andreas, Kampmann, and Mehring Le-Doare, 2015). A number of studies have reviewed the immunological advantages of breast milk against specific pathogens (viruses, bacteria, and parasites) as well as separate clinical illnesses (e.g. necrotizing enterocolitis, bacteremia, meningitis, respiratory tract illness, diarrheal disease, and otitis media) (R. A. Lawrence, 1997; R. M. Lawrence & Lawrence, 2004). The significance of breast milk for the newborns' immune system was recognized since ancient times according to the treatises of Hippocrates, Soranus and Galen, who advised breastfeeding from the mother or a wet-nurse (Fulminante, 2015).

Furthermore, according to the results of MixSIAR, the individuals that developed EH defects consumed more animal protein, most likely in the form of milk (Garnsey, 1999), compared to those who did not (Table 8). It is possible that these individuals were not only lacking the immunological advantages of breastmilk consumption but were also exposed to non-sterilized feeding vessels, which, especially in settings with poor hygiene, can increase the risk of infections (Kendall et al., 2021).

It is also important to consider that children can benefit from the nutritional characteristics of breast milk for a limited period (approximately for the first six months of age) (Kendall et al., 2021; Pérez-Escamilla, Buccini, Segura-Pérez, and Piwoz, 2019). As infants grow their nutritional expectations change and breast milk alone is not sufficient (Kendall et al., 2021). Although it is significant that supplementary sources of nutrition must be introduced, there is no guarantee that the nutritional quality of these foods is adequate. A possible explanation for the individuals we examined is that their diet was not nutritionally sufficient, and these children were severely malnourished.

Overall, we found diverse weaning practices in the site, which adhere to a baby-led weaning pattern (Cichero, 2016). Specifically, according to this pattern, parents provide the supplementary foods but the infant decides what they will eat, how much and how quickly (Cichero, 2016). This weaning pattern may prove harmful for some infants, such as premature ones, who have higher iron needs than term babies (Baker, Greer, and Committee on Nutrition American Academy of Pediatrics, 2010) and also have difficulty managing lumpy solids even at 12 months of age (Hawdon, Beauregard, Slattery, and Kennedy, 2000). Furthermore, the early introduction of solids may lead to the development of bad feeding behaviors, such as picky eating or skipping meals (Chung, Lee, Spinazzola, Rosen, and Milanaik, 2014), which overall increase the risk of malnutrition.

Methodological insights: histology and stable isotope analysis in the assessment of physiological stress during weaning

The combined results of histological and isotopic analysis highlight that the individuals in ancient Thessaloniki exhibited high levels of physiological stress. This was also discussed in Ganiatsou et al., (2023) that used a machine learning approach to identify inconsistent changes in isotopic ratios during weaning, which are related to malnutrition (Beaumont & Montgomery, 2016; Craig-Atkins, Towers, & Beaumont, 2018; Garland et al., 2018). According to their results, isotopic patterns related to physiological stress were identified in 21 individuals out of the 51 examined in total. In the present study we examined 13 out of the 21 individuals as the remaining had no available canine or incisor to sample (Table S1) and found that all 13 showed hypoplastic defects. As EH is a robust sign of developmental disturbances the overlap of the two conditions i.e. the inconsistent changes between carbon and nitrogen isotopic ratios and the presence of EH during infancy indicates a "powerful duo" for detecting physiological stress in archaeological populations. However, due to the small sample size of the present study, *conclusions are drawn with caution against overinterpretation of these results*.

Finally, this study underscored the importance of histological analysis in the investigation of EH, which despite of its destructive nature, yields, so far, unprecedented precision. Furthermore, this analysis provided the means to examine for the first time the average short periodicity of enamel and average growth rates between cuspal and imbricational enamel in the individuals of ancient Thessaloniki that showed significant differences, compared to other studies (Table S7) (Dąbrowski et al., 2021; Goodman and Rose, 1990; Krenz-Niedbała and Kozłowski, 2013; Lukasik and Krenz-

Niedbała, 2014; Reid and Dean, 2000). This underlines the significance of dental growth rates estimation, since fluctuations due to stress, environmental, dietary factors (Goodman and Rose, 1990), and even social status (Nakayama, 2016) can lead to inaccurate age-at-formation estimation of LEH defects (Goodman and Rose, 1990; Witzel et al., 2008). Dental developmental charts and regression equations based on macroscopic measurements (Goodman and Rose, 1990; Massler et al., 1941), although they offer the advantage of non-destructive methodology, they do not take into account the fluctuations of growth rates among the different tooth types, different populations and the cuspal enamel growth, leading to incorrect age estimation of up to 6-12 months of age (Dąbrowski et al., 2021; Goodman and Rose, 1990; Krenz-Niedbała and Kozłowski, 2013; Lukasik and Krenz-Niedbała, 2014; Reid and Dean, 2000).

Conclusions

The present study examined EH in individuals from ancient Thessaloniki and found that this condition was more frequently developed in infants consuming less than 50% of breast milk during weaning. This highlights the significant immunological support that breast milk provided in ancient times and protected infants from experiencing severe episodes of physiological stress. Nevertheless, these episodes were frequent, recurrent and severe in the site considering that almost 50% of the dataset (27/66 individuals) developed multiple hypoplastic defects. This is evident by the results of the histological analysis showing that hypoplastic defects, mostly of the linear type, occurred between the ages of 2.0-5.0 years and usually after the completion of weaning, consistent with other studies. Overall, the study employs a novel methodological approach to examine EH, and sheds light on a previously unexplored aspect on this condition. Our results, obtained from high-precision assays and statistical techniques, provide empirical data that support the heatedly debated causation of EH in ancient populations.

Acknowledgements

Elissavet Ganiatsou and Panagiota Bantavanou would like to thank the Committee of the Dental Anthropological Association for awarding this study at the 2023 Albert Dalberg Competition. The authors would like to extend their gratitude to the Ephorate of Antiquities of Thessaloniki City for entrusting the human skeletal material, to Christina Kakasa, Maria Christodoulou, and Eugenia Mantatzi from the Laboratory of Physical Anthropology DUTh for providing the anthropological data and to Nikos Vordos and Nikos Pradakis from the Hephaestus Advanced Laboratory of the International Hellenic University for authorizing and providing assistance for the usage of the micro -CT.

Funding

This research has been co-financed by the European Regional Development Fund of the European Union and Greek national funds through the Operational Program Competitiveness, Entrepreneurship and Innovation, under the call RESEARCH–CREATE–INNOVATE (project title: ECHOES- Development of a methodology for the digital reconstruction of ancient human biographies through the study of archeo-anthropolog-ical material, project code: T2EDK-00152). E.G and A.A were funded by Greece and the European Union (European Social Fund-ESF) through the Operational Programme "Human Resources Development, Education and Lifelong Learning" in the context of the Act "Enhancing Human Resources Research Potential by undertaking a Doctoral Research" Sub-action 2: IKY Scholarship Programme for PhD candidates in the Greek Universities».

References

Acheilara, L. (2007). Thessaloniki METRO 2007: The archaeological Work of the 16th Ephorate of Prehistoric and Classical Antiquities. In P. Adam-Veleni & K. Tzanavari (Eds.), *AEMTh 21* (pp. 215–222). Ministry of Culture.

Acheilara, L. (2008). Thessaloniki METRO 2008: The archaeological work of the 16th Ephorate of Prehistoric and Classical Antiquities. In P. Adam-Veleni & K. Tzanavari (Eds.), *AEMTh 22* (pp. 265–272). Ministry of Culture.

Acheilara, L. (2009). Thessaloniki METRO 2009: The archaeological Work of the 16th Ephorate of Prehistoric and Classical Antiquities. In P. Adam-Veleni & K. Tzanavari (Eds.), *AEMTh 23* (pp. 247–254). Ministry of Culture.

Acheilara, L. (2010). Thessaloniki METRO 2010: The work of the 16th Ephorate of Prehistoric and Classical Antiquities. In P. Adam-Veleni & K. Tzanavari (Eds.), *AEMTh 24* (pp. 217–222). Ministry of Culture.

Acheilara, L. (2011). Thessaloniki METRO 2011: archaeological research. In P. Adam-Veleni & K. Tzanavari (Eds.), *AEMTh 25* (pp. 309–316). Ministry of Culture.

Acsádi, G., Nemeskéri, J., & Balás, K. (1970). *History of human life span and mortality* (pp. 113–135).

Adam-Veleni, P. (2003). Thessalonike: history and town planning. In D. V. Grammenos (Ed.), *Roman Thessaloniki* (pp. 121–162). Hellenic Ministry of Culture - Archaeological Receipts Fund - Telloglion Art Foundation.

Adam-Veleni, P. (2012). Macedonia and Thessaloniki. In P. Adam-Veleni & D. Terzopoulou (Eds.), *Field.House.Garden.Grave*. Archaeological Museum of Thessaloniki.

Aldred, M., Talacko, A., & Steyn, N. (2016). Enamel Hypoplasia. In P. Slootweg (Ed.), *Dental and Oral Pathology* (pp. 149–152). Switzerland: Springer Reference.

Allamani-Souri, V. (2003). The province of Macedonia in the Roman Imperium. In D. V. Grammenos (Ed.), *Roman Thessaloniki* (pp. 67–79). Hellenic Ministry of Culture, Archaeological Receipts Fund, Telloglion Art Foundation.

AlQahtani, S. J., Hector, M. P., & Liversidge, H. M. (2010). Brief communication: The London atlas of human tooth development and eruption. *American Journal of Physical Anthropology*, 142 (3), 481–490.

Ambrose, S. H. (1990). Preparation and characterization of bone and tooth collagen for isotopic analysis. *Journal of Archaeological Science*, 17(4), 431–451.

Ambrose, S. H. (2002). Controlled Diet and Climate Experiments on Nitrogen Isotope Ratios of Rats. In S. H. Ambrose & M. A. Katzenberg (Eds.), *Biogeochemical Approaches to Paleodietary Analysis* (pp. 243–259). Boston, MA: Springer US.

Andreas, N. J., Kampmann, B., & Mehring Le-Doare, K. (2015). Human breast milk: A review on its composition and bioactivity. *Early Human Development*, 91(11), 629–635.

Antoine, D., FitzGerald, C. M., & Rose, J. C. (2018). Incremental Structures In Teeth. In *Biological Anthropology of the Human Skeleton* (pp. 225–256). John Wiley & Sons, Ltd.

Antoine, D., & Hillson, S. (2015). Enamel Structure and Properties. In *A Companion to Dental Anthropology* (pp. 223–243). John Wiley & Sons, Ltd.

Baker, R. D., Greer, F. R., & Committee on Nutrition American Academy of Pediatrics. (2010). Diagnosis and prevention of iron deficiency and iron-deficiency anemia in infants and young children (0-3 years of age). *Pediatrics*, 126(5), 1040–1050.

Bakirtzis, H., & Pazaras, N. (2006). Thessaloniki Metro 2006. *AEMTH 20*, 431–454. Hellenic Ministry of Culture.

Bakirtztis, H., & Pazaras, N. (2006). Thessaloniki Metro 2006. In P. Adam-Veleni & K. Tzanavari (Eds.), *AEMTh 20* (pp. 431–454). Hellenic Ministry of Culture.

Beaumont, J. (2020). The Whole Tooth and Nothing but the Tooth: Or why Temporal Resolution of Bone Collagen May Be Unreliable. *Archaeometry*, 62(3), 626–645.

Beaumont, J., & Montgomery, J. (2015). Oral histories: a simple method of assigning chronological age to isotopic values from human dentine collagen. *Annals of Human Biology*, 42(4), 407–414.

Beaumont, J., & Montgomery, J. (2016). The Great Irish Famine: Identifying Starvation in the Tissues of Victims Using Stable Isotope Analysis of Bone and Incremental Dentine Collagen. *PloS One*, 11(8), e0160065.

Blakey, M. L., Leslie, T. E., & Reidy, J. P. (1994). Frequency and chronological distribution of dental enamel hypoplasia in enslaved African Americans: a test of the weaning hypothesis. *American Journal of Physical Anthropology*, 95(4), 371–383.

Brooks, S., & Suchey, J. M. (1990). Skeletal age determination based on the os pubis: A comparison of the Acsádi-Nemeskéri and Suchey-Brooks methods. *Human Evolution*, 5(3), 227–238.

Brothwell, D. R. (1981). *Digging Up Bones: The Excavation, Treatment, and Study of Human Skeletal Remains*. Cornell University Press.

Brown, T. A., Nelson, D. E., Vogel, J. S., & Southon, J. R. (1988). Improved Collagen Extraction by Modified Longin Method. *Radiocarbon*, 30(2), 171–177.

Buikstra, J., & Ubelaker, D. (1994). Standards for Data Collection from Human Skeletal Remains. *Proceedings of a Seminar at The Field Museum of Natural History Organized by Jonathan Haas*. Arkansas Archaeological Survey Research Series No 44.

Caufield, P. W., Li, Y., & Bromage, T. G. (2012). Hypoplasia-associated Severe Early Childhood Caries – A Proposed Definition. *Journal of Dental Research*, 91(6), 544–550.

Chinique de Armas, Y., González Herrera, U. M., Reyes Serrano, I., Buhay, W. M., Skelton, S., Rodríguez Suárez, R., … Laffoon, J. (2022). Multiproxy paleodietary reconstruction using stable isotopes and starch analysis: The case of the archaeological site of Playa del Mango, Granma, Cuba. *Journal of Archaeological Science: Reports*, 46, 103671.

Chinique de Armas, Y., Roksandic, M., Nikitović, D., Rodríguez Suárez, R., Smith, D., Kanik, N.,

… Buhay, W. M. (2017). Isotopic reconstruction of the weaning process in the archaeological population of Canímar Abajo, Cuba: A Bayesian probability mixing model approach. *PloS One*, 12(5), e0176065.

Chung, J., Lee, J., Spinazzola, R., Rosen, L., & Milanaik, R. (2014). Parental perception of premature infant growth and feeding behaviors: use of gestation-adjusted age and assessing for developmental readiness during solid food introduction. *Clinical Pediatrics*, 53(13), 1271–1277.

Cichero, J. A. Y. (2016). Introducing solid foods using baby-led weaning vs. spoon-feeding: A focus on oral development, nutrient intake and quality of research to bring balance to the debate. *Nutrition Bulletin / BNF*, 41(1), 72–77.

Corruccini, R. S., Handler, J. S., & Jacobi, K. P. (1985). Chronological distribution of enamel hypoplasias and weaning in a Caribbean slave population. *Human Biology*, 57(4), 699–711.

Craig-Atkins, E., Towers, J., & Beaumont, J. (2018). The role of infant life histories in the construction of identities in death: An incremental isotope study of dietary and physiological status among children afforded differential burial. *American Journal of Physical Anthropology*, 167 (3), 644–655.

Cucina, A. (2002). Brief communication: diachronic investigation of linear enamel hypoplasia in prehistoric skeletal samples from Trentino, Italy. *American Journal of Physical Anthropology*, 119(3), 283–287.

Curtis, M. J., Beaumont, J., Elamin, F., Wilson, A. S., & Koon, H. E. C. (2022). Method of microsampling human dentine collagen for stable isotope analysis. *Rapid Communications in Mass Spectrometry: RCM*, 36(13), e9305.

Czermak, A., Fernández-Crespo, T., Ditchfield, P. W., & Lee-Thorp, J. A. (2020). A guide for an anatomically sensitive dentine microsampling and age-alignment approach for human teeth isotopic sequences. *American Journal of Physical Anthropology*, 173(4), 776–783.

Dąbrowski, P., Kulus, M., Grzelak, J., Radzikowska, M., Oziembłowski, M., Domagała, Z., & Krajcarz, M. T. (2020). Assessing weaning stress – Relations between enamel hypoplasia, δ18O and δ13C values in human teeth obtained from early modern cemeteries in Wroclaw, Poland. *Annals of Anatomy - Anatomischer Anzeiger*, 232, 151546.

Dąbrowski, P., Kulus, M. J., Furmanek, M., Paulsen, F., Grzelak, J., & Domagała, Z. (2021). Estimation of age at onset of linear enamel hypoplasia. New calculation tool, description and comparison of current methods. *Journal of Anatomy*, 239(4), 920–931.

Dean, C. M. (2017). How the microstructure of dentine can contribute to reconstructing developing dentitions and the lives of hominoids and hominins. *Comptes Rendus. Palevol*, 16(5), 557–571.

DeNiro, M. J. (1985). Postmortem preservation and alteration of in vivo bone collagen isotope ratios in relation to palaeodietary reconstruction. *Nature*, 317(6040), 806–809.

Dittmann, K., & Grupe, G. (2000). Biochemical and Palaeopathological Investigations on Weaning and Infant Mortality in the Early Middle Ages. *Anthropologischer Anzeiger; Bericht Uber Die Biologisch-Anthropologische Literatur*, 58(4), 345–355.

Dotsika, E., Diamantopoulos, G., Lykoudis, S., Gougoura, S., Kranioti, E., Karalis, P., … Palaigeorgiou, E. (2019). Establishment of a Greek Food Database for Palaeodiet Reconstruction: Case Study of Human and Fauna Remains from Neolithic to Late Bronze Age from Greece. *Geosciences Journal*, 9(4), 165.

Eerkens, J. W., Berget, A. G., & Bartelink, E. J. (2011). Estimating weaning and early childhood diet from serial micro-samples of dentin collagen. *Journal of Archaeological Science*, 38 (11), 3101–3111.

Eriksson, J. G., Kajantie, E., Osmond, C., Thornburg, K., & Barker, D. J. P. (2010). Boys live dangerously in the womb. *American Journal of Human Biology: The Official Journal of the Human Biology Council*, 22(3), 330–335.

Ferembach, D., Schwindezky, I., & Stoukal, M. (1980). Recommendation for Age and Sex Diagnoses of Skeletons. *Journal of Human Evolution*, 9, 517–549.

Fernandes, R., Grootes, P., Nadeau, M.-J., & Nehlich, O. (2015). Quantitative diet reconstruction of a Neolithic population using a Bayesian mixing model (FRUITS): The case study of Ostorf (Germany). *American Journal of Physical Anthropology*, 158(2), 325–340.

Fernández-Crespo, T., Schulting, R. J., Czermak, A., Ordoño, J., Lorenzo, J. I., & Rodanés, J. M. (2022). The "post-weanling's conundrum": exploring the impact of infant and child feeding practices on early mortality in the Bronze Age burial cave of Moro de Alins, north-eastern Iberia, through stable isotope analysis. *Archaeological and Anthropological Sciences*, 14(10), 196.

FitzGerald, C., Saunders, S., Bondioli, L., & Macchiarelli, R. (2006). Health of infants in an Imperial Roman skeletal sample: Perspective from dental microstructure. *American Journal of*

Physical Anthropology, 130(2), 179–189.

Fogel, M. L., Tuross, N., & Owsley, D. W. (1989). Nitrogen isotope tracers of human lactation in modern and archaeological populations. In *Carnegie Institution of Washington Yearbook* (pp. 111–117).

Fulminante, F. (2015). Infant Feeding Practices in Europe and the Mediterranean from Prehistory to the Middle Ages: A Comparison between the Historical Sources and Bioarchaeology. *Childhood in the Past*, 8(1), 24–47.

Galván, D. E., Sweeting, C. J., & Polunin, N. V. C. (2012). Methodological uncertainty in resource mixing models for generalist fishes. *Oecologia*, 169(4), 1083–1093.

Ganiatsou, E., Georgiadou, A., Souleles, A., Aidonis, A., Protopsalti, T., Tzevreni, S., … Papageorgopoulou, C. (2023). Application of Machine Learning on Isotopic Data from Tooth Microsections for Reconstructing Weaning Patterns and Physiological Stress. *Journal of Archaeological Science: Reports*, 47, 103765.

Ganiatsou, E., Souleles, A., & Papageorgopoulou, C. (2023). WEaning Age FiNder (WEAN): a tool for estimating weaning age from stable isotope ratios of dentinal collagen. *Archaeological and Anthropological Sciences*, 15(4), 50.

Ganiatsou, E., Vika, E., Georgiadou, A., Protopsalti, T., & Papageorgopoulou, C. (2022). Breastfeeding and Weaning in Roman Thessaloniki. An Investigation of Infant Diet based on Incremental Analysis of Human Dentine. *Environmental Archaeology*, 1–19.

Garland, C., Reitsema, L., Larsen, C. S., & Thomas, D. H. (2018). Early life stress at mission Santa Catalina de guale: An integrative analysis of enamel defects and dentin incremental isotope variation in malnutrition. *Bioarchaeology International*, 2(2), 75–94.

Garnsey, P. (1999). *Food and society in classical antiquity*. Cambridge University Press.

Goodman, A. H., & Armelagos, G. J. (1988). Childhood stress and decreased longevity in a prehistoric population. *American Anthropologist*, 90(4), 936–944.

Goodman, A. H., Armelagos, G. J., & Rose, J. C. (1984). The chronological distribution of enamel hypoplasias from prehistoric Dickson Mounds populations. *American Journal of Physical Anthropology*, 65(3), 259–266.

Goodman, A. H., & Rose, J. C. (1990). Assessment of systemic physiological perturbations from dental enamel hypoplasias and associated histological structures. *American Journal of Physical Anthropology*, 33(S11), 59–110.

Grueger, B., & Canadian Paediatric Society, Community Paediatrics Committee. (2013). Weaning from the breast. *Paediatrics & Child Health*, 18(4), 210–211.

Halcrow, S. E., Miller, M. J., Pechenkina, K., Dong, Y., & Fan, W. (2021). The bioarchaeology of infant feeding. *The Routledge Handbook of Anthropology and Reproduction*, 541–558.

Hawdon, J. M., Beauregard, N., Slattery, J., & Kennedy, G. (2000). Identification of neonates at risk of developing feeding problems in infancy. *Developmental Medicine and Child Neurology*, 42(4), 235–239.

Herrscher, E., Goude, G., & Metz, L. (2017). Longitudinal Study of Stable Isotope Compositions of Maternal Milk and Implications for the Palaeo-Diet of Infants. *Bulletins et Memoires de La Societe d'anthropologie de Paris*, 29(3–4), 131–139.

Hillson, S., & Bond, S. (1997). Relationship of enamel hypoplasia to the pattern of tooth crown growth: a discussion. *American Journal of Physical Anthropology*, 104(1), 89–103.

Hossin, M. Z. (2021). The male disadvantage in life expectancy: can we close the gender gap? *International Health*, 13(5), 482–484.

Hurnanen, J., Visnapuu, V., Sillanpää, M., Löyttyniemi, E., & Rautava, J. (2017). Deciduous neonatal line: Width is associated with duration of delivery. *Forensic Science International*, 271, 87–91.

Internationale, Fédération Dentaire. (1982). An epidemiological index of developmental defects of dental enamel (DDE Index). Commission on Oral Health, Research and Epidemiology. *International Dental Journal*, 32(2), 159–167.

Işcan, M. Y., Loth, S. R., & Wright, R. K. (1984). Age estimation from the rib by phase analysis: white males. *Journal of Forensic Sciences*, 29(4), 1094–1104.

Işcan, M. Y., Loth, S. R., & Wright, R. K. (1985). Age estimation from the rib by phase analysis: white females. *Journal of Forensic Sciences*, 30 (3), 853–863.

Kanonidis, I., Lamprothanasi, E., & Protopsalti, S. (2016). Thessaloniki's Metro 2016. The Work of the Ephorate of Antiquities of the city of Thessaloniki. From the precassandrian settlement of Pylaia to the centre of the ancient Thessaloniki. *AEMTh 30*, 301–310.

Karamberi, M. (2000). I autokratoriki edra sti Thessaloniki. *Thessalonikeon Polis*, 87–94.

Karamberi, M. (2003). The transformation of the residential character of southeast Thessaloniki. *Archaeological Work in Macedonia and Thrace*.

Katzenberg, M. A., & Herring, D. A. (1996). Weaning and infant mortality: evaluating the skeletal evidence. *American Journal of Physical Anthropology*, 101, 177–199.

Kendall, E., Millard, A., & Beaumont, J. (2021). The “weanling’s dilemma” revisited: Evolving bodies of evidence and the problem of infant paleodietary interpretation. *American Journal of Physical Anthropology*, 175 Suppl 72(S72), 57–78.

Krenz-Niedbała, M., & Kozłowski, T. T. (2013). Comparing the Chronological Distribution of Enamel Hypoplasia in Rogowo, Poland (2nd century AD) Using Two Methods of Defect Timing,. *International Journal of Osteoarchaeology*, 23, 410–442.

Larsen, C. S. (1987). 6 - Bioarchaeological Interpretations of Subsistence Economy and Behavior from Human Skeletal Remains. In M. B. Schiffer (Ed.), *Advances in Archaeological Method and Theory* (pp. 339–445). San Diego: Academic Press.

Lawrence, R. A. (1997). *A Review of the Medical Benefits and Contraindications to Breastfeeding in the United States*. National Center for Education in Maternal and Child Health.

Lawrence, R. M., & Lawrence, R. A. (2004). Breast milk and infection. *Clinics in Perinatology*, 31 (3), 501–528.

Lewis, M. (2018). Dental Disease, Defects, and Variations in Dental Morphology. *Paleopathology of Children*, 67–89.

Lovejoy, C. O., Meindl, R. S., Pryzbeck, T. R., & Mensforth, R. P. (1985). Chronological metamorphosis of the auricular surface of the ilium: A new method for the determination of adult skeletal age at death. *American Journal of Physical Anthropology*, 68(1), 15–28.

Lukasik, S., & Krenz-Niedbała, M. (2014). Age of linear enamel hypoplasia formation based on Massler and colleagues’ and Reid and Dean’s standards in a Polish sample dated to 13th-18th century CE. *Homo: Internationale Zeitschrift Fur Die Vergleichende Forschung Am Menschen*, 65(4), 296–310.

Makri, E., & Vasileiadou, S. (2011). Thessaloniki METRO 2008. The archaeological work of the 9th Ephorate of Byzantine Antiquities. *AEMTh 22*, 297–306.

Martin, S. A., Guatelli-Steinberg, D., Sciulli, P. W., & Walker, P. L. (2008). Brief communication: Comparison of methods for estimating chronological age at linear enamel formation on anterior dentition. *American Journal of Physical Anthropology*, 135(3), 362–365.

Mary, H., & Brouhard, G. J. (2019). Kappa (κ): Analysis of Curvature in Biological Image Data using B-splines. *BioRxiv*. doi:10.1101/852772

Massler, M., Schour, I., & Poncher, H. G. (1941). Developmental pattern of the child as reflected in the calcification of the teeth. *American Journal of Diseases of Children* , 62(1), 33–67.

McElreath, R. (2020). *Statistical rethinking: A Bayesian course with examples in R and Stan*. Chapman and Hall/CRC.

Miles, A. E. W. (1962). Assessment of the Ages of a Population of Anglo-Saxons from Their Dentitions. *Proceedings of the Royal Society of Medicine*, 55(10), 881–886.

Misailidou-Despotidou, V. (2012). Thessaloniki’s Metro 2012. The work of IST’ EPKA. *AEMTh* 26, 291–304.

Misailidou-Despotidou, V., Lamprothanasi, E., & Protopsalti, S. (2014). Thessaloniki’s Metro 2014. *AEMTh* 28, 291–301.

Miszkiewicz, J. J. (2015). Linear Enamel Hypoplasia and Age-at-Death at Medieval (11th–16th Centuries) St. Gregory’s Priory and Cemetery, Canterbury, UK. *International Journal of Osteoarchaeology*, 25(1), 79–87.

Moggi-Cecchi, J., Pacciani, E., & Pinto-Cisternas, J. (1994). Enamel hypoplasia and age at weaning in 19th-century Florence, Italy. *American Journal of Physical Anthropology*, 93(3), 299–306.

Moore, J. W., & Semmens, B. X. (2008). Incorporating uncertainty and prior information into stable isotope mixing models. *Ecology Letters*, 11 (5), 470–480.

Nigdelis, P. M. (1997a). Apo ton Kassandro ston Galerio: Schediasma istorias tis archaias Thessalonikis. *Thessalonikeon Polis*, 21–29.

Nigdelis, P. M. (1997b). From Casander to Galerius: sketching the history of ancient Thessaloniki. *Thessalonikeon Polis*, 1, 21–29.

Nikakis, D. (2019). *Hellenistic and roman jewellery: the finds from metro excavations at the east and west cemetery of ancient Thessaloniki*. Aristotle University of Thessaloniki.

Paisidou, M., Vasileiadou, S., & Konstantinidou, K. (2009). Thessaloniki METRO 2010: The work of the 9th Ephorate of Byzantine Antiquities. *AEMTh* 23, 255–266.

Pérez-Escamilla, R., Buccini, G. S., Segura-Pérez, S., & Piwoz, E. (2019). Perspective: Should Exclusive Breastfeeding Still Be Recommended for 6 Months? *Advances in Nutrition*, 10(6), 931–943.

Phenice, T. W. (1969). A newly developed visual method of sexing the os pubis. *American Journal of Physical Anthropology*, 30(2), 297–301.

Phillips, D. L. (2001). Mixing models in analyses of diet using multiple stable isotopes: a critique. *Oecologia*, 127(2), 166–170.

Pitsios, T. (2012). Frequency and Distribution of Enamel Hypoplasia in Ancient Skulls from Different Eras and Areas in Greece. *International Journal of Caring Sciences*, 5.

Reid, D. J., Beynon, A. D., & Ramirez Rozzi, F. V. (1998). Histological reconstruction of dental development in four individuals from a medieval site in Picardie, France. *Journal of Human Evolution*, 35(4), 463–477.

Reid, D. J., & Dean, M. C. (2000). Brief communication: The timing of linear hypoplasias on human anterior teeth. *American Journal of Physical Anthropology*, 113(1), 135–139.

Reid, D. J., & Dean, M. C. (2006). Variation in modern human enamel formation times. *Journal of Human Evolution*, 50(3), 329–346.

Risnes, S. (1986). Enamel apposition rate and the prism periodicity in human teeth. *European Journal of Oral Sciences*, 94(5), 394–404.

Ritzman, T. B., Baker, B. J., & Schwartz, G. T. (2008). A fine line: A comparison of methods for estimating ages of linear enamel hypoplasia formation. *American Journal of Physical Anthropology*, 135(3), 348–361.

Roberts, C., & Manchester, K. (2010). *The archaeology of disease*.

Sandberg, P. A., Sponheimer, M., Lee-Thorp, J., & Van Gerven, D. (2014). Intra-tooth stable isotope analysis of dentine: A step toward addressing selective mortality in the reconstruction of life history in the archaeological record. *American Journal of Physical Anthropology*, 155 (2), 281–293.

Sarnat, B. G., & Schour, I. (1941). Enamel Hypoplasia (Chronologic Enamel Aplasia) in Relation to Systemic Disease: A Chronologic, Morphologic and Etiologic Classification. *The Journal of the American Dental Association*, 28(12), 1989–2000.

Schwarcz, H. P. (1991). Some theoretical aspects of isotope paleodiet studies. *Journal of Archaeological Science*, 18(3), 261–275.

Seow, W. K. (2017). Etiology of developmental enamel defects in the primary dentition. *Clinical Dentistry Reviewed*, 1(1), 7.

Skinner, M., & Anderson, G. S. (1991). Individualization and enamel histology: a case report in forensic anthropology. *Journal of Forensic Sciences*, 36(3), 939–948.

Smith, T. (2020). Dental Histology. *Archaeological Science An Introduction*, 170–197.

Stock, B. C., Jackson, A. L., Ward, E. J., Parnell, A. C., Phillips, D. L., & Semmens, B. X. (2018). Analyzing mixing systems using a new generation of Bayesian tracer mixing models. *PeerJ*, 6, e5096.

Tagiguchi, H. (1966). Chronologic relationship of human tooth crown formation. *The Journal of Nihon University School of Dentistry*, 40, 391–397.

Tomczyk, J., Tomczyk-Gruca, M., & Zalewska, M. (2012). Frequency and chronological distribution of linear enamel hypoplasia (LEH) in the Late Neolithic and Early Bronze Age population from Żerniki Górne (Poland) – preliminary report. *Administrative Radiology: AR*, 75(1), 61–73.

Vakalopoulos, A. (1983). *History of Thessaloniki 316 B.C - 1983* (p. 153). Thessaloniki: Stamoulis Publications.

van Klinken, G. J. (1999). Bone Collagen Quality Indicators for Palaeodietary and Radiocarbon Measurements. *Journal of Archaeological Science*, 26(6), 687–695.

Vasileiadou, S., & Pazaras, N. (2010). Thessaloniki metro, 2007. In P. Adam-Veleni & K. Tzanavari (Eds.), *AEMTh 21*. Hellenic Ministry of Culture.

Vehtari, A., Gelman, A., & Gabry, J. (2017). Practical Bayesian model evaluation using leave-one -out cross-validation and WAIC. *Statistics and Computing*, 27(5), 1413–1432.

Witzel, C., Kierdorf, U., Schultz, M., & Kierdorf, H. (2008). Insights from the inside: histological analysis of abnormal enamel microstructure associated with hypoplastic enamel defects in human teeth. *American Journal of Physical Anthropology*, 136(4), 400–414.

Wong, C., Schreiber, V., Crawford, K., & Kumar, S. (2023). Male infants are at higher risk of neonatal mortality and severe morbidity. *The Australian & New Zealand Journal of Obstetrics & Gynaecology*. doi:10.1111/ajo.13689

Dental Anthropology

Volume 37, Issue 01, 2024

Research Articles

Variation in Regional Enamel Growth Rates in Modern Humans Presenting Dental Evidence of Vitaimin D Deficiency
Christopher Aris, Katie A. Hemer, and Emma Street 3

An Investigation of Enamel Hypoplasia and Weaning through Histomorphological Analaysis and Bayesian Isotope Mixing Models
Panagiota Bantavanou, Elissavet Ganiatsou, Angelos Souleles, Angeliki Georgiadou, Panagiota Xanthopoulou, Asterios Aidonis, and Christina Papageorgopoulou 20

Published at:
Western Carolina University
1 University Drive, Cullowhee, North Carolina, 28723 U.S.A.
Western Carolina University is an EEO/AA employer